Monthly Notices
of the
ROYAL ASTRONOMICAL SOCIETY

Mon. Not. R. Astron. Soc. **400,** 1347–1365 (2009) doi:10.1111/j.1365-2966.2009.15440.x

# Chemical evolution of local galaxies in a hierarchical model

F. Calura[1,2]★ and N. Menci[3]

[1]*Dipartimento di Astronomia-Universitá di Trieste, via G.B. Tiepolo 11, 34131 Trieste, Italy*
[2]*INAF, Osservatorio Astronomico di Trieste, via G.B. Tiepolo 11, 34131 Trieste, Italy*
[3] *INAF, Osservatorio Astronomico di Roma, via Frascati 33, I-00040 Monteporzio, Italy*

Accepted 2009 July 22. Received 2009 July 21; in original form 2009 March 12

**ABSTRACT**

We investigate the chemical properties of local galaxies within a cosmological framework in the hierarchical picture of galaxy formation. To this aim, we use a hierarchical semi-analytic model which includes the contribution from (i) low- and intermediate-mass stars, relevant producers of some important elements, such as C and N; (ii) Type Ia supernovae (SNe), for which a continuous delay-time distribution is assumed and which are important for the production of Fe and (iii) massive stars, dying as core-collapse Type II SNe and which produce the $\alpha$ elements. In this way, we can study abundances for a large set of chemical elements and in various galactic types, comparing our predictions with available observations in the Milky Way (MW), in local dwarf galaxies and in local ellipticals.

For MW-like galaxies, we can successfully reproduce the major observational constraints, i.e. the [O–Fe] versus [Fe/H] relation observed in disc stars and the stellar metallicity distribution (SMD). For dwarf galaxies, the stellar metallicity versus mass relation is reproduced by assuming that a substantial fraction of the heavy elements is lost through metal-enhanced outflows and a Type Ia SN realization probability lower than the one of MW-like galaxies. The predicted abundance ratios for dwarf galaxies are comparable to observations derived locally for dwarf spheroidals. The SMDs predicted for dwarf galaxies are in agreement with the local observations. We predict a substantial presence of extremely low metallicity stars [Fe/H] $< -2.5$, which have been recently observed in ultrafaint dwarf galaxies. In ellipticals, the observations indicate higher [$\alpha$/Fe] values in larger galaxies. Several previous attempts to model the [$\alpha$/Fe] versus $\sigma$ in ellipticals based on $\Lambda$ cold dark matter galaxy formation models predicted an anticorrelation between [$\alpha$/Fe] versus $\sigma$, indicating too much extended star formation histories in high-mass galaxies. Our results computed with a standard Salpeter initial mass function (IMF) indicate a flat [$\alpha$/Fe] versus $\sigma$ relation. However, we suggest a possible solution to this problem and show how, by assuming a star-formation-dependent IMF with a slope $x = 1.35$ in systems with star formation rates $<100\,\mathrm{M}_{\odot}\,\mathrm{yr}^{-1}$ and slightly flatter (i.e. with $x = 1$) in object with stronger star formation, the observed correlation between [$\alpha$/Fe] and $\sigma$ can be accounted for on a large velocity dispersion range. Fundamental roles are played also by interaction-triggered starbursts and active galactic nuclei feedback. Finally, a star-formation-dependent IMF seems necessary also to reproduce the stellar metallicity–$\sigma$ relation observed in local early-type galaxies.

**Key words:** galaxies: abundances – galaxies: evolution – galaxies: formation.

## 1 INTRODUCTION

In the last few years, the power of high-resolution spectrographs has made available a large amount of stellar and interstellar abundances for various chemical species. Nowadays, large catalogues of stellar abundances are accessible for the Milky Way (MW) galaxy and for the dwarf galaxies of the Local Group. Gas-phase abundances have been derived up to high redshift ($z > 3$), both by analysing emission lines and absorption lines, present in the spectra of distant quasars. This large set of data provides us with valuable constraints for galactic chemical evolution studies. Of particular interest is the study of chemical evolution by means of *ab initio* galaxy formation models.

★E-mail: fcalura@oats.inaf.it

The study of galactic chemical evolution within a cosmological framework is of particular importance, since it provides us with crucial information on the star formation history (SFH) of galaxies, on the ages of the stellar populations and on the gas accretion and outflow histories. Chemical evolution offers a way to constrain the main parameters driving all of these processes, which are of primary interest for galaxy formation theories.

So far, a few theoretical studies of hierarchical galaxy formation have paid attention to the problem of galactic chemical evolution. In a pioneeristic paper, Thomas (1999) considered SFHs from a hierarchical semi-analytic galaxy formation model, taking into account for the first time the rates of Type Ia supernovae (SNe). This attempt allowed him to compute the evolution of the abundance ratio between elements formed on different time-scales, i.e. O, synthesized by Type II SNe on time-scales less than 0.03 Gyr, and Fe, produced mainly by Type Ia SNe on time-scales ranging from 0.03 Gyr up to one Hubble time. Other important works on chemical evolution in the hierarchical framework are the ones by Nagashima et al. (2005), and Nagashima & Okamoto (2006), where the chemical evolution of various elements produced by Type Ia and Type II SNe is computed. However, none of the works quoted above takes into account the role of low- and intermediate-mass stars (LIMS), i.e. all the stars with masses $0.8 \leq m/\mathrm{M}_{\odot} \leq 8$. These stars are of fundamental importance in chemical evolution studies since they incorporate an important fraction of the metals and during the last stages of their evolution, i.e. during the planetary nebula phase, they may restore variable amounts of non-processed heavy elements incorporated at their birth and produced by stars of previous generations, giving a significant contribution to the heavy element pollution of the interstellar medium (ISM). Furthermore, LIMS are relevant producers of C and N (van den Hoek & Groenewegen 1997), whose abundances cannot be properly assessed by any chemical evolution model which does not take into account in detail the evolution of LIMS. In this paper, with a hierarchical semi-analytical model (SAM) we study the chemical evolution of these heavy elements, taking into account also the contribution from LIMS. Our main aim is providing chemical evolution predictions computed by means of star formation (SF) and gas accretion histories derived from an *ab initio* galaxy formation model. For the first time, by means of a SAM for galaxy formation, we study the evolution of the abundances for a large set of chemical elements produced by stars of various masses, ending their lives on various time-scales. This paper is mainly focused on the chemical abundances in local galaxies. We compare our predictions to abundances observed in various galactic environments, such as in the MW disc, local dwarf galaxies and local early-type galaxies. Future papers will be devoted to the study of chemical abundances at high redshift. This paper is organized as follows. In Section 2, we present our theoretical instruments, i.e. the hierarchical semi-analytical galaxy formation model and the main chemical evolution equations. In Section 3, we present our results. Finally, in Section 4 we discuss the main implications of our results and draw some conclusions.

## 2 THE MODEL

In this paper, we start from the SFHs of galaxies computed by means of a semi-analytic model of galaxy formation. For each SFH, we compute the chemical evolution a posteriori by means of detailed chemical evolution equations. In this section, we briefly describe the SAM used in this work and the methods used to compute the evolution of the chemical abundances.

### 2.1 The galaxy formation model

We derive the SFHs of galaxies and of their progenitors from the SAM by Menci et al. (2006, 2008); we recall here its key features. Galaxy formation and evolution is driven by the collapse and growth of dark matter (DM) haloes, which originate by gravitational instability of overdense regions in the primordial DM density field. This is taken to be a random, Gaussian density field with cold dark matter (CDM) power spectrum within the 'concordance cosmology' (Spergel et al. 2007) for which we adopt round parameters $\Omega_{\Lambda} = 0.7, \Omega_0 = 0.3$, baryonic density $\Omega_{\mathrm{b}} = 0.04$ and Hubble constant (in units of $100\,\mathrm{km\,s^{-1}\,Mpc^{-1}}$) $h = 0.7$. The normalization of the spectrum is taken to be $\sigma_8 = 0.9$ in terms of the variance of the field smoothed over regions of $8\,h^{-1}\,\mathrm{Mpc}$.

As cosmic time increases, larger and larger regions of the density field collapse, and eventually lead to the formation of groups and clusters of galaxies, which grow by merging with mass- and redshift-dependent rates provided by the extended Press–Schechter formalism (see Bond et al. 1991; Lacey & Cole 1993). The clumps included into larger DM haloes may survive as satellites, or merge to form larger galaxies due to binary aggregations, or coalesce into the central dominant galaxy due to dynamical friction; these processes take place on time-scales that grow longer over cosmic time, so the number of satellite galaxies increases as the DM host haloes grow from groups to clusters. All the above processes are implemented in our model as described in detail in Menci et al. (2005, 2006), based on canonical prescriptions of semi-analytic modelling.

#### *2.1.1 Star formation and SN feedback*

The radiative gas cooling, the ensuing SF and the SN events with the associated feedback occurring in the growing DM haloes (with mass $M$ and circular velocity $v$) are described in Menci et al. (2005). The cooled gas with mass $M_{\mathrm{g}}$ settles into a rotationally supported disc with radius $r_{\mathrm{d}}$ (typically ranging from 1 to 5 kpc), rotation velocity $v_{\mathrm{d}}$ and dynamical time $t_{\mathrm{d}} = r_{\mathrm{d}}/v_{\mathrm{d}}$. The gas gradually condenses into stars and the stellar feedback returns part of the cooled gas to the hot gas phase with mass $M_{\mathrm{h}}$ at the virial temperature of the halo. As for the SF, we assume the canonical Schmidt form $\psi = M_{\mathrm{g}}/(q\tau_{\mathrm{d}})$, where $\tau_{\mathrm{d}} \equiv r_{\mathrm{d}}/v_{\mathrm{d}}$ and $q$ is fixed by the Kennicutt (1998) law. At each time-step, the mass $\Delta m_{\mathrm{h}}$ returned from the cold gas content of the disc to the hot gas phase due to SNe activity is estimated from canonical energy balance arguments (Kauffmann 1996; Kauffmann & Charlot 1998; see also Dekel & Birnboim 2006) as

$$\Delta m_{\mathrm{h}} = E_{\mathrm{SN}}\,\epsilon_0\,\eta_0\,\Delta m_*/v_{\mathrm{c}}^2, \qquad (1)$$

where $\Delta m_*$ is the mass of stars formed in the time-step, $\eta \approx 3$–$5 \times 10^{-3}\,\mathrm{M}_{\odot}^{-1}$ is the number of SNe per unit solar mass [depending on the assumed initial mass function (IMF)], $E_{\mathrm{SN}} = 10^{51}$ erg is the energy of ejecta of each SN and $v_{\mathrm{c}}$ is the circular velocity of the galactic halo; $\epsilon_0 = 0.01$–$0.5$ is the efficiency of the energy transfer to the cold interstellar gas. The above mass $\Delta\, m_{\mathrm{h}}$ is made available for cooling at the next time-step. The model free parameters $q = 30$ and $\epsilon_0 = 0.1$ are chosen as to match the local $B$-band luminosity function and the Tully–Fisher relation adopting a Salpeter IMF.

Note that our simple modelling for SNe feedback provides a very good fit to the observed correlations of outflow velocities with galactic properties [like the circular velocity or the star formation rate (SFR)]. Although an accurate estimate of the outflow velocity would require a detailed treatment of the gas kinematics (including also the physics of OB associations and the dynamics of superbubbles; see Ferrara, Pettini & Shchekinov 2000; Veilleux, Cecil &

Bland-Hawthorn 2005) and is beyond the aim of the present paper, its asymptotic value $V_{\rm outflow}$ can be estimated from the energetic balance between the total energy deposition rate by SNe and the rate of kinetic energy loss as (Veilleux et al. 2005) $\Delta\, m_{\rm h}\, V^2_{\rm max} = E_{\rm SN}\, \epsilon_0\, \eta_0\, \psi$. A comparison with our assumed expression for the expelled gas mass $\Delta\, m_{\rm h}$ given above implies $V_{\rm max} \approx v_{\rm c}$ (or equivalently a mass loading factor $\dot{m}_{\rm h}/\psi \propto v_{\rm c}^{-2}$), a relation which is in very good agreement with the relation observed in local starbursts (Martin 2005; Rupke, Veilleux & Sanders 2005; Veilleux, Cecil & Bland-Hawthorn 2005).

#### 2.1.2 AGN feedback

The model also includes a treatment of the growth of supermassive black holes at the centre of galaxies by interaction-triggered inflow of cold gas, following the physical model of Cavaliere & Vittorini (2000). Our SAM includes a detailed treatment of feedback from active galactic nuclei (AGN), which acts only during the active AGN phases of each galaxy (hence for a minor fraction $\sim 10^{-2}$ of the galaxy lifetime). This is assumed to stem from the fast winds with velocity up to $10^{-1}c$ observed in the central regions of AGN (Weymann 1981; Turnshek et al. 1988; Risaliti et al. 2005); these are usually though to originate from the acceleration of disc outflows due to the AGN radiation field (Proga 2007 and references therein). These supersonic outflows compress the gas into a blast wave terminated by a leading shock front, which moves outwards with a lower but still supersonic speed and sweeps out the surrounding medium. Eventually, this is expelled from the galaxy. Quantitatively, the energy injected into the galactic gas in such inner regions is taken to be proportional to the energy radiated by the AGN, $\Delta E = \epsilon_{\rm AGN}\, \eta\, c^2\, \Delta m_{\rm acc}$. The value of the energy feedback efficiency for coupling with the surrounding gas is taken as $\epsilon_{\rm AGN} = 5 \times 10^{-2}$, consistent with the values required to match the X-ray properties of the intracluster medium (ICM) in clusters of galaxies (see Cavaliere, Lapi & Menci 2002). This is also consistent with the observations of wind speeds up to $v_{\rm w} \approx 0.1c$ in the central regions, that yield $\epsilon_{\rm AGN} \approx v_{\rm w}/2c \approx 0.05$ by momentum conservation between photons and particles (see Chartas et al. 2002; Pounds et al. 2003); this value has been also adopted in a number of simulations (e.g. Di Matteo, Springel & Hernquist 2005) and SAMs of galaxy formation (e.g. Menci et al. 2006). The transport of the above energy in the galaxy and its effect on the distribution of the galactic gas is computed in detail by describing the expansion of the blast wave solving the corresponding hydrodynamical equations; these include the effects not only of initial density gradient, but also those of upstream pressure and DM gravity (Lapi, Cavaliere & Menci 2005). The solutions show in detail how the perturbed gas is confined to an expanding shell bounded by an outer shock at the radius $R_{\rm s}(t)$ which sweeps out the gas surrounding the AGN. From the resulting shock expansion law $R_{\rm s}(t)$ the amount of expelled gas can be computed (for different AGN luminosities and galactic properties), as well as the final galactic gas distribution, as described in detail in Menci et al. (2008). We refer to Menci et al. (2005, 2006, 2008) for details and for the comparison of the model results with observations concerning the cosmological evolution of both the galaxy and the AGN population.

#### 2.1.3 Starbursts triggered by galaxy interactions

An additional channel for SF implemented in the model is provided by interaction-driven starbursts, triggered not only by merging but also by fly-by events between galaxies; such a SF mode provides an important contribution to the early formation of stars in massive galaxies, as described in detail in Menci et al. (2004, 2005). The galaxy interaction rate is given by $\tau_{\rm r}^{-1} = n_{\rm T}\, \Sigma(r_{\rm t},\, v,\, V_{\rm rel})\, V_{\rm rel}$, where $n_{\rm T}$ is the number of galaxies hosted in a given DM halo, $\Sigma$ is the cross-section for grazing (i.e. at distances closer than the galaxy tidal radius) encounters, computed as in Menci et al. (2002) from the orbital parameters (the impact parameter $b$, the radius of the host DM halo) for each galaxy in our Monte Carlo simulations; the relative velocity $V_{\rm rel}$ is computed from the velocity dispersion of the DM halo hosting the interacting galaxies. With a probability given by the above equation in each time-step, a galaxy is considered to be in a starburst phase. In such a case, the cold gas fraction converted into stars during the burst is $f_{\rm acc} \approx |\Delta j/j| = 10^{-1}\, \langle (m'/m)\, (r_{\rm d}/b)\, (v_{\rm d}/V_{\rm rel}) \rangle$ . The fraction of cold gas accreted by the black hole in an interaction event is here computed in terms of the variation $\Delta\, j$ of the specific angular momentum $j \approx Gm/v_{\rm d}$, induced by the grazing encounter. Here $m'$ is the mass of the partner galaxy in the interaction, and the average runs over the probability of finding such a galaxy in the same halo where the galaxy with mass $m$ is located. The duration of the burst is given by the interaction time-scale $r_{\rm d}/V_{\rm rel}$. With such a description, a fraction of gas $\approx$ 10 per cent is impulsively converted into stars during minor bursts with $m'/m \approx 0.1$, while in the rarer major bursts with $m'/m \approx 1$ the fraction of gas converted into stars can approach 100 per cent.

### 2.2 Galactic chemical evolution

In this paper, we model chemical evolution following the approach of Matteucci & Greggio (1986). We follow the time evolution of the abundances for the following set of chemical elements: H, He, C, N, O, Mg, Si, Fe. This is one of the major novelties of this work, since so far such a large set of chemical elements has never been considered in SAMs for galaxy formation.

For any chemical element $i$, the variation of its mass in the interstellar gas per unit time is

$$\frac{{\rm d}m_i}{{\rm d}t} = -X_i(t)\psi(t) + R_{{\rm LIMS},i}(t) + R_{{\rm Ia},i}(t) + R_{{\rm II},i}(t) + I_i(t) + O_i(t), \quad (2)$$

where $X_i$ is the mass fraction in the gas for the element $i$ at the time $t$, $\psi(t)$ is the SFR of the selected galaxy. The terms $R_{{\rm LIMS},i}(t)$, $R_{{\rm Ia},i}(t)$ and $R_{{\rm II},i}(t)$ are the rates of production of the element $i$ from stars of low and intermediate mass, Type Ia and Type II SNe, respectively.

Finally, the terms $I_i(t)$ and $O_i(t)$ take into account possible mass increments and outflows of mass in the form of the element $i$, respectively. The mass increment may occur by means of three processes: (i) cooling of hot gas; (ii) by means of cool gas accretion or (iii) merging with other galaxies, whereas an outflow can occur owing to a galactic wind. In the remainder of the paper, when we will use the expression 'infall', we will intend actually the increment of gas, which can occur by means of any of the three processes mentioned above. The methods used to compute the accretion and outflow histories of the galaxies will be described in Section 2.3.

Stars of low and intermediate mass are those with initial masses $0.8 \leq m/{\rm M}_\odot \leq 8$. Their production rate for the element $i$ is given by

$$R_{{\rm LIMS},i}(t) = \int_{0.8}^{M(t)} \psi(t - \tau_m) m_{{\rm LIMS},i}(m) \phi(m)\, {\rm d}m, \quad (3)$$

where $M(t)$ is the turnoff mass at the time $t$, $\tau_m$ is the lifetime of the star of mass $m$, $\phi(m)$ is the IMF and $m_{\mathrm{LIMS},i}(m)$ is the total mass in the form of the element $i$ that a LIMS restores into the ISM.

Unless otherwise stated, for the IMF, we assume a Salpeter (1955) law, given by $\phi(m) = C\, m^{-(1+x)}$ with $x = 1.35$. The constant $C$ is determined by the condition

$$\int_{0.1}^{100} m\, \phi(m)\, \mathrm{d}m = 1, \tag{4}$$

i.e. from the normalization to one of the IMF by mass. The quantities $m_{\mathrm{LIMS},i}(m)$ are taken from van den Hoek & Groenewegen (1997), who computed theoretical yields for various elements and for stars of low and intermediate mass as a function of the initial metallicity $Z$. The yield $p_i(m)$ is defined as the fraction of the initial mass that a star transforms into the chemical element $i$ and restores into the ISM. The quantity $m_{\mathrm{LIMS},i}(m)$ is computed from the yield according to

$$m_{\mathrm{LIMS},i}(m) = X_i(t - \tau_m) m_{\mathrm{ej}}(m) + m\, p_i(m), \tag{5}$$

where $X_i(t - \tau_m)$ and $m_{\mathrm{ej}}(m)$ are the original abundance of the element $i$ computed at the time $t - \tau_m$, i.e. when the star of mass $m$ formed, and the total ejected mass for a star of initial mass $m$, respectively.

For the element $i$, the production rate by Type Ia SNe is $R_{\mathrm{Ia},i}(t) = m_{\mathrm{Ia},i}\ R_{\mathrm{Ia}}(t)$. $R_{\mathrm{Ia}}(t)$ is the Type Ia SN rate at the time $t$, computed according to

$$R_{\mathrm{Ia}}(t) = k_\alpha A_{\mathrm{Ia}} \int_{\tau_i}^{\min(t,\tau_x)} \psi(t - \tau) \mathrm{DTD}(\tau)\, \mathrm{d}\tau \tag{6}$$

(Greggio 2005; Matteucci et al. 2006). The quantity $k_\alpha$ is the number of stars per unit mass in a stellar generation, given by

$$k_\alpha = \int_{m_l}^{M_L} \phi(m)\, \mathrm{d}m, \tag{7}$$

where $m_l = 0.1\,\mathrm{M}_\odot$ and $M_L = 100\,\mathrm{M}_\odot$, whereas $A_{\mathrm{Ia}}$ is the realization probability for Type Ia SNe and represents the fraction of binary systems which may give rise to Type Ia SNe, assumed to be constant in time. This quantity is uncertain (Maoz 2008) and is likely to depend on the environment (Matteucci et al. 2006). In chemical evolution studies, $A_{\mathrm{Ia}}$ is basically treated as a free parameter, tuned in order to reproduce the Type Ia SN rate in local galaxies (see Calura & Matteucci 2006; Matteucci et al. 2006). We will test the impact of this parameter on some of the results described in this paper.

The function DTD ($\tau$) is the delay time distribution. We assume that Type Ia SNe originate from the explosion of a C/O white dwarf (WD) in a close binary system, where the companion is either a red giant or a main-sequence star. This is the single-degenerate (SD) model of Whelan & Iben (1973). The DTD ($\tau$) is from Matteucci et al. (2006, see also Matteucci 2001; Valiante et al. 2009).

$m_{\mathrm{Ia},i}$ is the mass that a Type Ia SN synthesizes and ejects into the ISM in the form of the element $i$. These quantities are taken from Iwamoto et al. (1999).

We assume that all stars with mass $m \geq 8\,\mathrm{M}_\odot$ explode as Type II SNe. The rate of production of the element $i$ from Type II SNe is

$$R_{\mathrm{II},i}(t) = \int_8^{100} \psi(t - \tau_m) m_{\mathrm{II},i}(m) \phi(m)\, \mathrm{d}m \simeq \psi(t) \int_8^{100} m_{\mathrm{II},i}(m) \phi(m)\, \mathrm{d}m. \tag{8}$$

The above simplification means to assume the instantaneous recycling approximation to treat chemical enrichment from massive stars, i.e. to assume that all stars with masses $m \geq 8\,\mathrm{M}_\odot$ have very small lifetimes. This assumption is motivated by the fact that the time-step we use to compute chemical evolution is of $\sim$0.015 Gyr, i.e. half the lifetime of a massive star of $8\,\mathrm{M}_\odot$. With such a time-step, the effects of the lifetimes of single massive stars of various masses cannot be appreciated.

Chemical enrichment from Type II SNe is computed by means of the quantity $m_{\mathrm{II},i}$:

$$m_{\mathrm{II},i}(m) = m_{\mathrm{II,new},i} + m_{\mathrm{ej}}\, X_i(t), \tag{9}$$

where

$$m_{\mathrm{II,new},i} = p_i(m) m. \tag{10}$$

The second term on the right-hand side of equation (9) is the mass in the form of the element $i$ already present when the star formed: $m_{\mathrm{ej}}$ is the total mass ejected by a star of mass $m$ and $X_i$ is the interstellar mass fraction of the element $i$ at the time $t$. For massive stars, we adopt the metallicity-dependent yields of Woosley & Weaver (1995).

### 2.3 Determining the past star formation, accretion and the outflow history

For any galaxy at redshift $z \sim 0$, it is possible to reconstruct its SFR $\psi(t)$ and its accretion and outflow histories on the basis of its past merging history. We have already described the possible gas accretion processes in Section 2.2. The outflows may originate owing to the contribution of SN explosions and of the AGN feedback. As described in Sections 2.1.1 and 2.1.2, both mechanisms inject energy into the ISM and cause gas to move from the cold phase to the hot phase. The hot gas may eventually be ejected if its thermal energy is larger than its binding energy, due to the gravitational well of both the DM and the baryons. For a particular galaxy, its SFR at a past time $t$ is given by

$$\psi(t) = \Sigma_j \psi_j(t), \tag{11}$$

where $\psi_j(t)$ is the SFR of the $j$th progenitor of the galaxy at the time $t$. This formula allows us to take into account the complex merging history of galaxies, playing an important role in chemical evolution. In a similar way, at any past time $t$, for any galaxy we are able to determine the total cold gas mass $M_{\mathrm{g}}(t)$. If $\Delta_{\mathrm{gas}}(t) = M_{\mathrm{g}}(t + \mathrm{d}t) - M_{\mathrm{g}}(t) - \Sigma_i\, R_{*,i}\, \mathrm{d}t + \psi(t)\, \mathrm{d}t$ is the difference in the total gas mass at two following time-steps minus the total mass restored by the stars in $\mathrm{d}t$ plus the mass ending in stars, we use this quantity to compute the total 'increment' and outflow rate at any time-step. If $\Delta_{\mathrm{gas}}(t)\, \mathrm{M}_\odot^{-1} > 0$, then we assume that at the time $t$,

$$I(t) = \Delta_{\mathrm{gas}}/\mathrm{d}t, \qquad O(t) = 0; \tag{12}$$

otherwise

$$I(t) = 0, \qquad O(t) = \Delta_{\mathrm{gas}}(t)/\mathrm{d}t. \tag{13}$$

By means of these quantities, we are able to solve the chemical evolution equations described in Section 2.2. For any chemical element $i$, $I_i(t) = X_i(t)\, I(t)$ in case of merging or $I_i(t) = X_{i,\mathrm{p}}(t)\, I(t)$ in case of infall of pristine gas, where $X_{i,\mathrm{p}}$ is the primordial mass fraction for the element $i$.

In the SAM, the metal-enriched gas expelled from satellite galaxies residing in a common DM halo is diluted by the hot gas of the halo, whose amount is much larger, generally by a factor of 100, than the amount of the interstellar cold gas. For this reason, the metallicity of the gas which may eventually fall back from the hot

halo on to a galaxy, which in general is the central galaxy of the halo, may be considered negligible. This allows us to assume that the accreted gas has a primordial composition, i.e. $X_{\rm H,p} = 0.75$, $X_{\rm He,p} = 0.25$ and for any other element, we assume $X_{i,\rm p} = 0$. On the other hand, for any element, unless otherwise stated, we assume $O_i(t) = X_i(t)\, O(t)$, i.e. the chemical composition of the outflow is the same as the one of the cold ISM.

## 3 RESULTS

In this section, we describe the results obtained for various types of galactic systems. These results concern mainly local galaxies and are compared to observational constraints obtained in the MW, in local dwarf galaxies and in local ellipticals. A study of the chemical evolution of distant galaxies is the subject for future work.

At $z \sim 0$, from the catalogue of galaxies obtained by means of the SAM of Menci et al. (2008), we select galaxies on the basis of various criteria. The selection criteria are similar to those adopted for the observations, and are based on the combined use of various available quantities, such as the colour, SFR or the stellar mass. In the following sections, we describe how we select galaxies of various types and our comparison with observational data from the literature.

### 3.1 Chemical abundances in Milky-Way-like galaxies

The first important step of our study is to test our predictions for MW-like galaxies. Recently, De Rossi et al. (2009) published a detailed study of MW-like galaxies extracted from the Millennium Simulation catalogue. Following De Rossi et al. (2009), we define MW-like galaxies as those with circular velocity $V_{\rm c}$ in the range $200 < V_{\rm c}\,{\rm km^{-1}\,s^{-1}} < 240$ and cold gas fractions $f_{\rm c} = M_{\rm g}/(M_{\rm g} + M_*)$ in the range $0.1 \leq f_{\rm c} \leq 0.3$.

By means of these criteria, for the local number density of MW-like galaxies, we obtain $\sim 1 \times 10^{-4}\,{\rm Mpc^{-3}}$, consistent with De Rossi et al. (2009).

In Fig. 1, we show the SFHs of a set of nine MW-like galaxies drawn from our sample. In Fig. 2, we show the cumulative stellar and gas masses as a function of time for these galaxies, whereas in Fig. 3 we show the time evolution of the gas accretion rates.

The predicted abundance ratios between any chemical element and Fe are sensitive to the parameters we have assumed to describe the Type Ia SN rate. In particular, having assumed in this case a Salpeter IMF constant in time, the most relevant parameter in this study is the Type Ia realization probability $A_{\rm Ia}$. In the literature, this quantity is not well constrained, but it is generally considered as a free parameter tuned in order to reproduce the local Type Ia SN rate (Calura & Matteucci 2006; Matteucci et al. 2006). In Fig. 4, we show the present-time Type Ia SN rate, expressed in SNuM,[1] predicted for our selected MW-like galaxies and compared to an observational range for the MW global Type Ia SN rate. The observational range is computed by assuming a SN rate of 0.3–0.4 century$^{-1}$ (van & Tammann 1991) and a present day disc stellar mass of $\sim 5 \times 10^{10}\,{\rm M_\odot}$ (Mera et al. 1998). This figure shows that the assumption of a Type Ia SN frequency $A_{\rm Ia} = 0.002$ provides present day Type Ia SN rates in reasonable agreement with the observations (upper panel of Fig. 4) whereas by assuming $A_{\rm Ia} = 0.004$ we severely overestimate the observed Type Ia SN rate (lower panel of Fig. 4). From this moment on, $A_{\rm Ia} = 0.002$ be our reference value for the Type Ia SN realization probability.

[1] 1 SNuM = 1 SN century$^{-1}$ $10^{-10}\,{\rm M_\odot^{-1}}$.

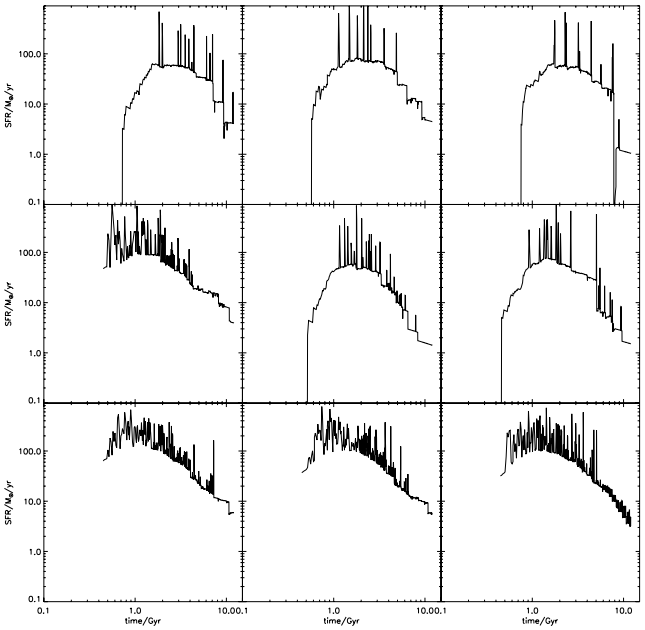


**Figure 1.** SFHs of a few MW-like galaxies selected according the criteria described in Section 3.1.

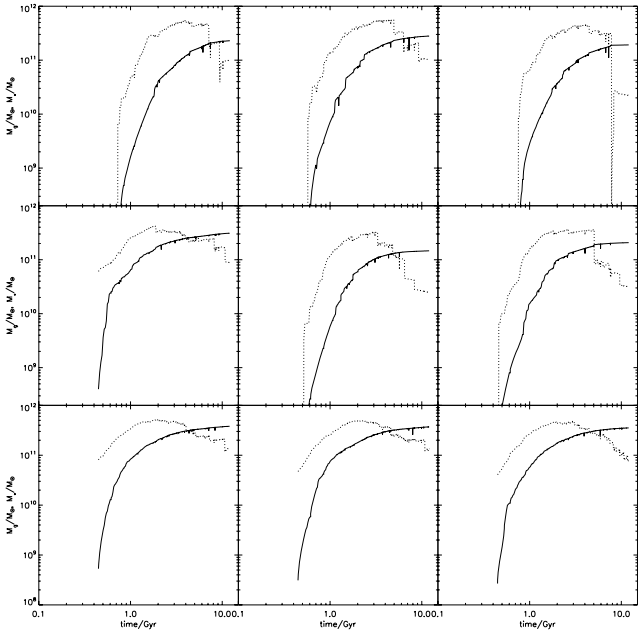


**Figure 2.** Evolution of the cumulative stellar masses (solid lines) and gas masses (dotted lines) for a few MW-like galaxies selected according the criteria described in Section 3.1.

The chemical abundances obtained for the galaxies selected according to the criteria described at the beginning of this section are now compared to the abundances observed in MW stars.

In Fig. 5, we show the predicted abundance ratios versus metallicity for our sample of MW-like galaxies, compared to a set of observations of abundance ratios in MW stars for various elements. The predictions are represented by the colour code at the top of Fig. 5, expressing the predicted number of stellar populations belonging to galaxies with given abundance ratio at metallicity [Fe/H],

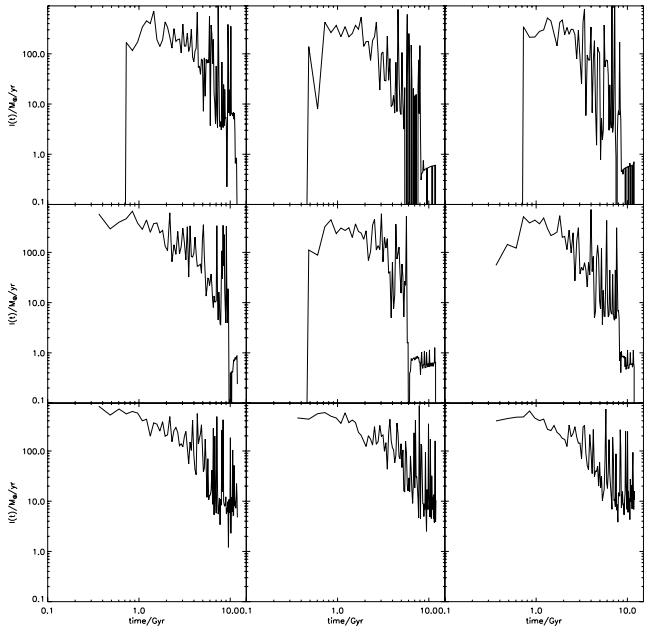


**Figure 3.** Time evolution of the increment rate $I(t)$ for a few MW-like galaxies selected according the criteria described in Section 3.1.

normalized to the total number of stellar populations at that metallicity. The symbols are the observational values from several sources (for further details, see caption of Fig. 5). In Fig. 5, the observational data are single-star abundances, i.e. each point represents the abundance ratios observed in a single local star. On the other hand, in our model we cannot resolve single stars, hence we consider the average abundances in a stellar population and we compare them to observations. For each selected MW-like galaxy, in the time interval d$t$ a stellar mass d$M_*$ will be formed, characterized by a given metallicity (i.e. [Fe/H]) and particular abundance ratios. In Fig. 5, the coloured regions represent the predicted [X/Fe]–[Fe/H] distributions computed considering each stellar population of mass d$M_*$ born in each selected MW-like galaxy. This is very similar to what is done in chemical evolution models for the solar neighbourhood (see Matteucci 2001), barring the fact that in that case single tracks, representing the predictions for one single SFH, are plotted in the [X/Fe]–[Fe/H] diagrams. In our case, instead of having one single evolutionary track, we have various model tracks, each one drawn from a particular SFH for a MW-like galaxy. All these tracks populate the coloured areas of Fig. 5.

It is important to note that we cannot explore the metallicity region [Fe/H] $\leq -2.5$. To study chemical evolution at metallicities lower than this value, it would be necessary to consider finite stellar lifetimes also for massive stars. However, the metallicity range $-2.5 \leq$ [ Fe/H ] $\leq 0$ encompasses the Fe abundances of all thin and thick disc stars, hence it is useful to investigate the chemical evolution of MW-like galaxies during their major disc phases. In Fig. 5, in the [O/Fe] versus [Fe/H] plot the predictions indicate the presence of two main populations of stars. The first population has the [O/Fe] ratio in anticorrelation with the [Fe/H] and overlaps with the observation of local stars. Beside this, Fig. 5 shows the presence of a horizontal population of stars with metallicity $-2 \leq$ [Fe/H] $\leq -0.2$ and constant [O/Fe] $\sim -0.3$. A similar behaviour is visible also in the [C/Fe]–[Fe/H], [Mg/Fe]–[Fe/H] and [Si/Fe]–[Fe/H] plots. This is due to substantial late increment episodes, very frequent in selected MW-like galaxies (see Fig. 3). The late accretion of pristine gas has the effect of decreasing the metallicity [Fe/H] of

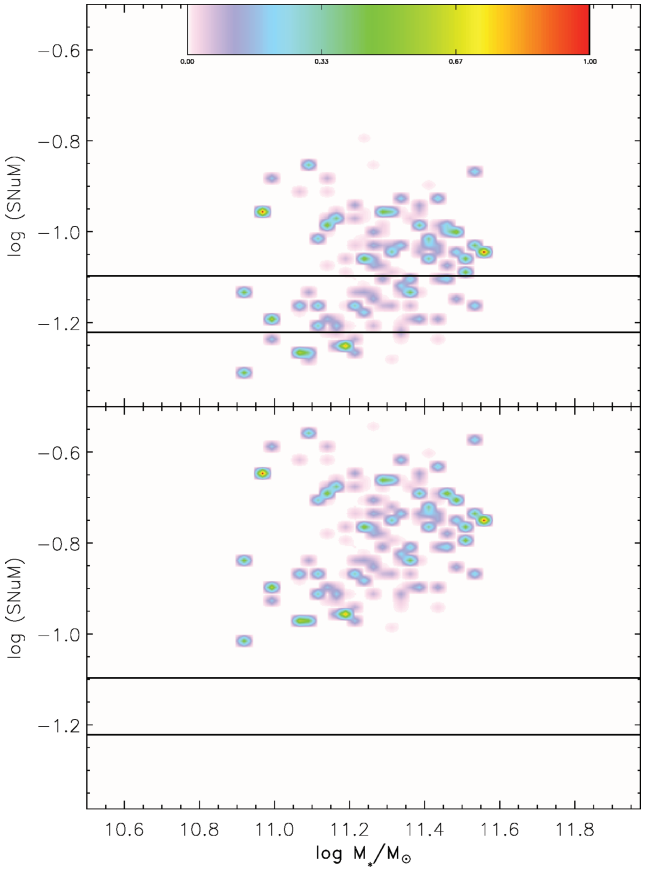


**Figure 4.** Predicted Type Ia SN rate, expressed in SNuM (1 SNuM = 1 SN century$^{-1}$ $10^{-10}$ $M_\odot^{-1}$) for selected MW-like galaxies compared to an estimate of the Type Ia SN rate for the MW (black solid lines). The colour code, shown by the bar at the top of the figure, represents the predicted number of galaxies with a given SNuM and a stellar mass $M_*$, normalized to the total number of galaxies with that stellar mass. In the upper and lower panels, the SN rate is computed by assuming $A_{\rm Ia} = 0.002$ and 0.004, respectively.

each stellar population born immediately after the infall event, having little effect on the [O/Fe] ratio, since both O and Fe are diluted by the same amount. Note that none of the observational data in Fig. 5 shows this peculiar behaviour. To better understand this point, in Fig. 6 we show for one of the selected MW-like galaxies the time evolution of the average interstellar [$\alpha$/Fe] and [Fe/H], of the total infall rate and the [$\alpha$/Fe] versus [Fe/H] diagram. From the [Fe/H] versus time and infall versus time plots, one can clearly see that in correspondence of two major gas accretion episodes at 7.5 and $\sim$11 Gyr, the [Fe/H] drops abruptly whereas the [$\alpha$/Fe] remains unchanged. In the [$\alpha$/Fe]–[Fe/H] diagram, the late accretion episodes and the consequent decrease of interstellar [Fe/H] are visible in the 'turn-off' of the track at [Fe/H] $\sim 0$, where the curve bends back towards lower [Fe/H], at constant [$\alpha$/Fe] $\sim -0.5$. The decrease of [Fe/H] at constant [$\alpha$/Fe] stops at [Fe/H] $\sim -1.7$, where the track bends forward, moving towards higher [Fe/H] values.

To investigate this point, we perform a further selection on the sample of MW-like galaxies. The basic reason of the presence of the horizontal population of stars in the [O/Fe]–[Fe/H] is late accretion episodes. Now we focus on a given redshift, in order to understand which fraction of the present day mass must be assembled in galaxies presenting chemical features the most similar to those of the MW as possible. This test may be useful to give constraints on the

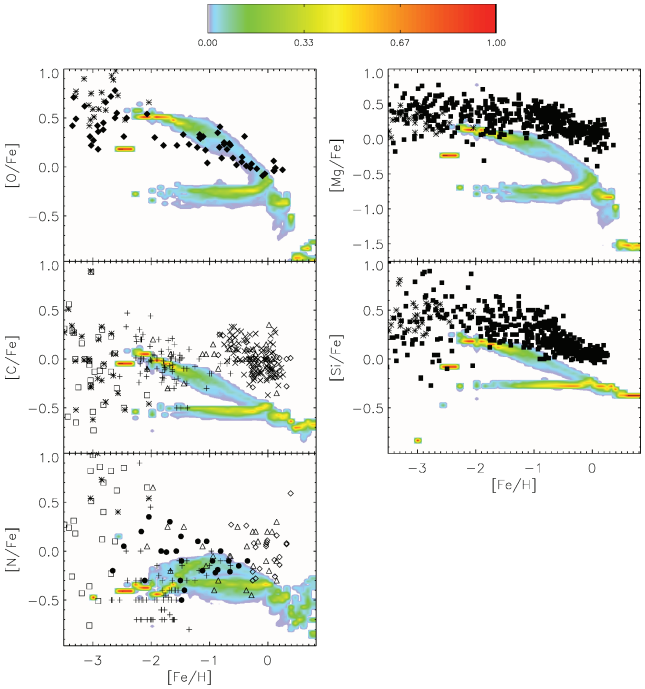


**Figure 5.** Predicted distribution of the abundance ratios [X/Fe] versus [Fe/H] for selected MW-like galaxies for several chemical elements compared with observations from various authors. The colour code, shown by the bar at the top of the figure, represents the predicted number of stellar populations belonging to MW-like galaxies with a given abundance ratio at metallicity [Fe/H], normalized to the total number of stellar populations at that metallicity. Observational data: asterisks: Cayrel et al. (2004); plus signs: Carbon et al. (1987); open squares: Spite et al. (2005); open triangles: Laird (1985a,b); the crosses: Tomkin et al. (1995); open diamonds: Clegg, Lambert & Tomkin (1981); solid circles: Israelian et al. (2004); solid diamonds: François et al. (2004) and finally the solid squares are from a compilation of data by Cescutti (2008).

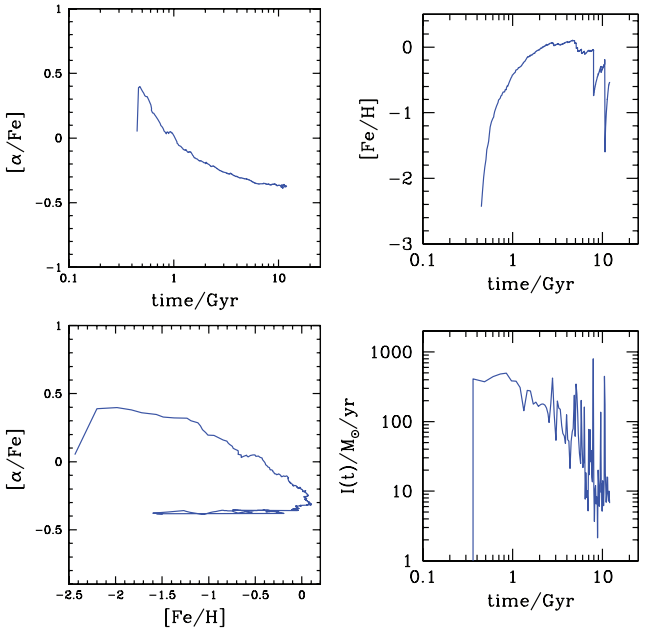


**Figure 6.** From top-left, clockwise: [$\alpha$/Fe] versus time, [Fe/H] versus time, infall rate versus time and [$\alpha$/Fe] versus [Fe/H] for one of the selected MW-like galaxies discussed in Section 3.1.

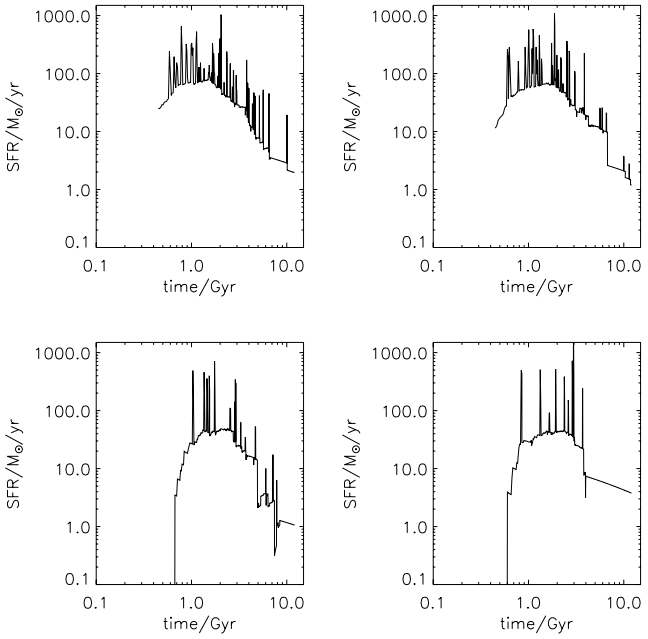


**Figure 7.** SFHs of MW-like galaxies whose mass assembled at $z = 2$ is at least 75 per cent of their present mass.

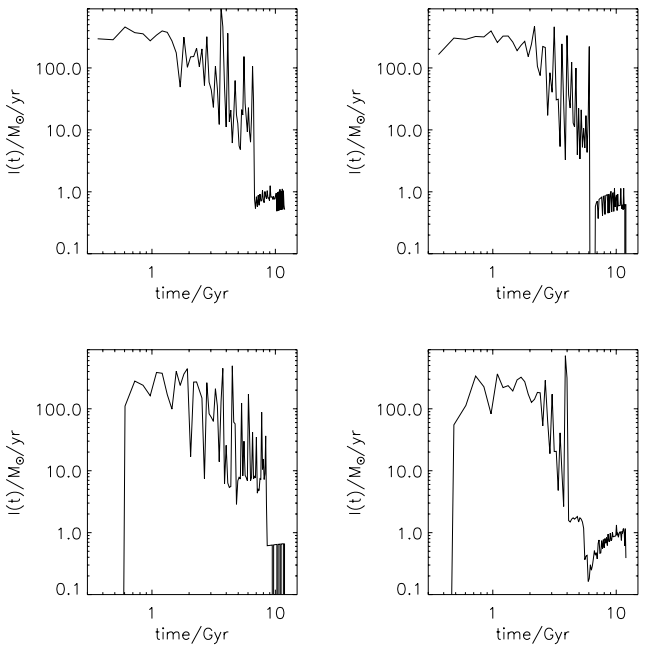


**Figure 8.** Time evolution of the increment rate $I(t)$ for MW-like galaxies whose assembled mass at $z = 2$ is at least 75 per cent of their present mass.

gas accretion history of the MW galaxy. We may focus on $z = 2$, which may be used as a lower limit to the highest redshift of major merging for MW-like galaxies (see e.g. Colavitti, Matteucci & Murante 2008). It is necessary that at least 75 per cent of the present day mass must be assembled at $z = 2$, in order to have the horizontal population vanished. In Fig. 7, we show the SF histories of these galaxies selected on the basis of their accretion history. The accretion histories of these galaxies are shown in Fig. 8. Basically, these galaxies do not experience major accretion episodes at epochs after ∼6 Gyr, at variance with most of the systems represented in Fig. 3, whereas their SFHs show low SFRs at late times. In Fig. 9,

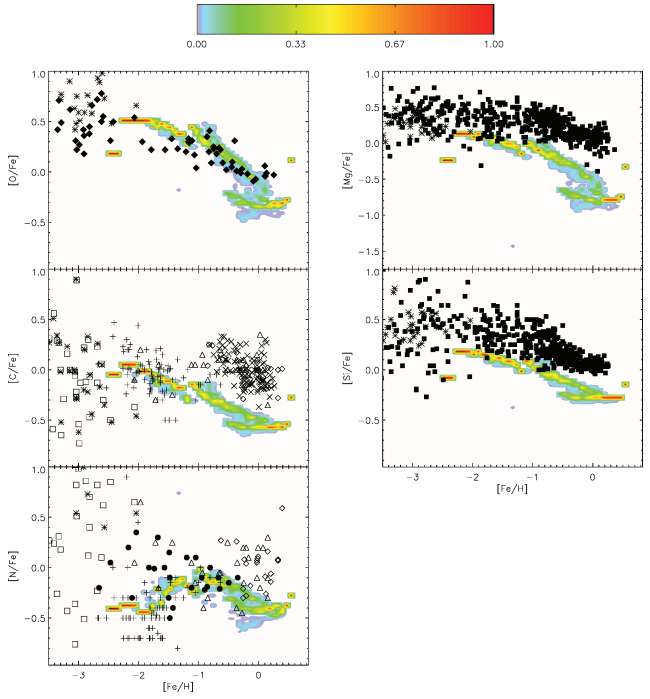


**Figure 9.** Predicted distribution of the abundance ratios [X/Fe] versus [Fe/H] for MW-like galaxies whose mass assembled at $z = 2$ is at least 75 per cent of their present mass for several chemical elements, compared with observations from various authors. The colour code, shown by the bar at the top of the figure, represents the predicted number of stellar populations belonging to MW-like galaxies born with a given abundance ratio and with metallicity [Fe/H], normalized to the total number of stellar populations with that metallicity. Observational data as in Fig. 5.

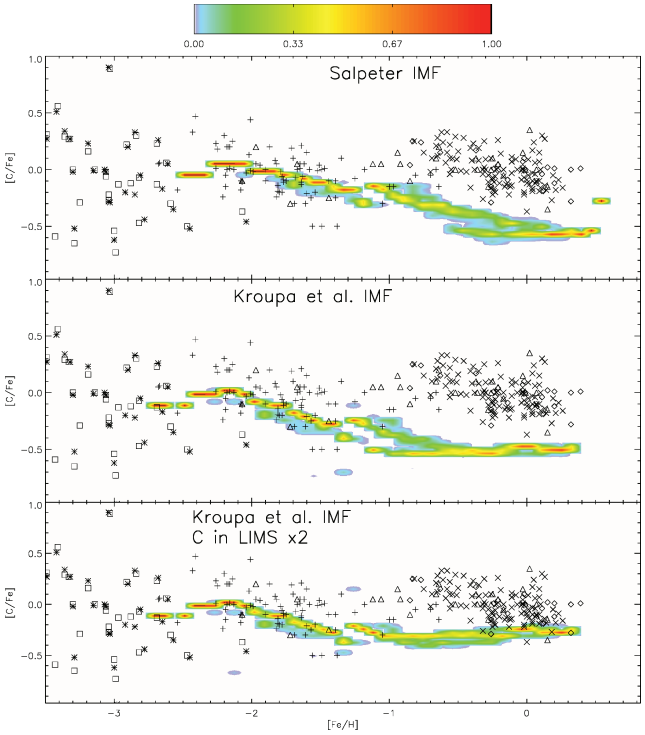


**Figure 10.** Effects of varying the stellar yields and the IMF on the predicted [C/Fe] versus [Fe/H] for selected MW-like galaxies. We show our results obtained assuming a Salpeter IMF and the standard stellar yields described in Section 2.2 (upper panel), a Kroupa et al. (1993) IMF and standard yields (middle panel), a Kroupa et al. (1993) IMF and the C yields of low and intermediate stars increased by a factor of 2. Colour code and observational data as in Fig. 5.

we show the predicted abundance ratios versus metallicity for all these galaxies. From Fig. 9, we see that in most of the cases, the observed behaviour of the abundance ratios measured in MW stars is satisfactorily reproduced.

Our results suggest that the abundance ratios observed in the MW stars exclude that our Galaxy experienced major pristine gas accretion episodes within the last few Gyr, either due to merging with gas-rich, low-metallicity dwarf galaxies, or due to infall of pristine gas.

Our results are in agreement with a large set of previous papers, indicating that the merging history of the MW must be completed at early times and that no significant infall episode took place in the last few Gyr, most of them based on the theoretical interpretation of abundances observed in MW disc and halo stellar populations or present-day properties of the MW galaxy (Prantzos & Silk 1998; Boissier & Prantzos 1999; Alibes, Labay & Canal 2001; Chiappini, Matteucci & Romano 2001; Hernandez, Avila-Reese & Firmani 2001; Naab & Ostriker 2006; Colavitti, Matteucci & Murante 2008; De Lucia & Helmi 2008) and on kinematical arguments (e.g. Gilmore, Wyse & Norris 2002; Wyse 2009).

In Fig. 9, the fact that for a few elements the predictions are shifted downwards with respect to the observed abundance ratios is mainly due to uncertainties related to the stellar yields used here. The [Mg/Fe] decreases by about 1.5 dex instead of less than 0.5 dex from [Fe/H] $= -2$ to $\sim 0$. Concerning the elements Mg and Si, it is well known from chemical evolution studies that the yields of Woosley & Weaver (1995) used here tend to underestimate the [Mg/Fe]–[Fe/H] and [Si/Fe]–[Fe/H] relations. François et al. (2004) reproduced the local observed abundance pattern by means of a model for the solar neighbourhood, increasing the yields of Mg by a factor of 7 and the yields of Si by a factor of 2, only for stars with masses $m > 40\,\mathrm{M}_{\odot}$ (see also Timmes, Woosley & Weaver 1995). Also the adopted C yields do not appear to be sufficient for reproducing the zero-point of the observed [C/Fe]–[Fe/H] relation and we underestimate the [C/Fe] on the whole metallicity range. Furthermore, the observed [C/Fe] exhibits a flat behaviour throughout the whole [Fe/H] range, whereas the SAM results show a remarkable anticorrelation. This may be certainly due to the adopted stellar yields, but also the IMF is likely to play some role in the predicted [X/Fe]–[Fe/H] relations. In Fig. 10, we show how different assumptions regarding the IMF and the stellar yields may affect our predictions in the [C/Fe]–[Fe/H] plot. With a Salpeter IMF and standard yields, our match to the data is very poor. The use of a Kroupa, Tout & Gilmore (1993) IMF causes a flattening of the predicted [C/Fe]–[Fe/H] at metallicities [Fe/H] $> -1$. This is due to the fact that with the Kroupa IMF the relative fraction of intermediate-mass stars, i.e. stars with masses $2 \leq M/\mathrm{M}_{\odot} \leq 8$, representing the most important C producers, is larger than with the Salpeter. If we assume a Kroupa et al. (1993) IMF and we artificially increase the yields of intermediate-mass stars by a factor 2, all the predictions at metallicity [Fe/H] $> -1$ shift upwards and overall the predicted [C/Fe]–[Fe/H] becomes flatter, in better agreement with the observations.

Romano et al. (2005) showed in detail the relative roles of the stellar yields and of the IMF in determining the abundance ratios, suggesting that the Salpeter IMF is not appropriate to reproduce most local chemical evolution constraints. However, a detailed investigation of the stellar yields and of the stellar IMF requires a fine-tuning of these parameters and is beyond the aims of the

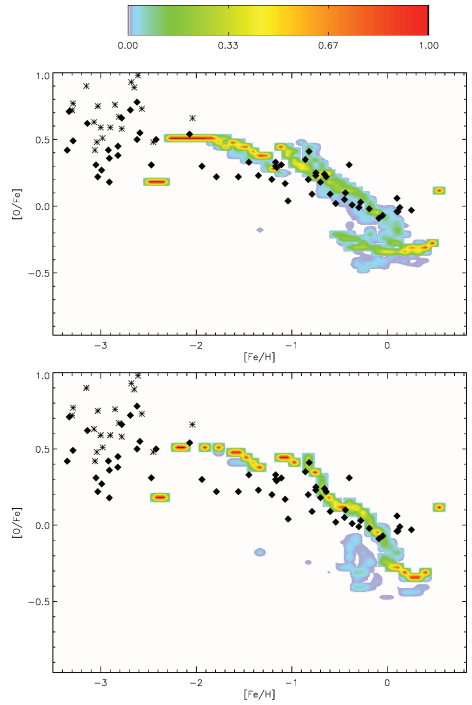


**Figure 11.** Predicted [O/Fe] versus [Fe/H] for MW galaxies selected on the basis of their gas accretion history (upper panel) and for the ones presenting a ratio between the stellar mass in the disc and total stellar mass $M_{*,\mathrm{d}}/M_{*,\mathrm{tot}} =$ 0.7–0.8 (lower panel). Colour code and observational data as in Fig. 5.

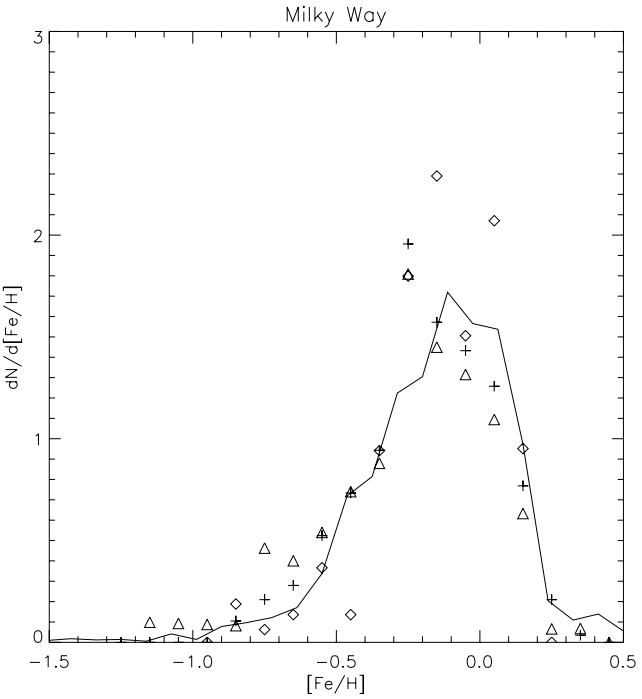


**Figure 12.** Predicted cumulative SMD of selected MW-like galaxies (solid line) compared to local observations from various authors. The model predictions and the observational data are normalized by imposing that the subtended areas have all the same value, equal to unity. Observations are from Wyse & Gilmore (1995): crosses; Rocha-Pinto & Maciel (1996): triangles and Jorgensen (2000): diamonds.

present paper, which is instead focused on the chemical evolution of galaxies within a cosmological framework.

We have verified that the use of a morphological criterion to select MW-like galaxies has a minor impact on our results. Among our sample of galaxies matching the chemical properties of MW-like galaxies, we can calculate the ratio between the stellar mass in the disc and the total stellar mass $M_*$ in the following way. The neutral gas mass of the MW disc is $\sim 1 \times 10^{10}\,\mathrm{M}_\odot$ (Carroll & Ostlie 1996; Prantzos & Silk 1998), whereas the stellar mass is $\sim 5 \times 10^{10}\,\mathrm{M}_\odot$, with a ratio between the gas mass and the stellar mass ∼0.2. We use this value to estimate the stellar mass in the disc of our selected MW-like galaxies, which is, since all the cold gas is in the disc, $M_{*,\mathrm{d}} = M_{\mathrm{g}}/0.2$. By assuming that the stellar mass of the MW bulge is 1–2 $\times$ $10^{10}\,\mathrm{M}_\odot$ (Reshetnikov 2000; Ballero et al. 2008), the observed disc-to-total stellar mass ratio is $M_{*,\mathrm{d}}/M_{*,\mathrm{tot}} = 0.7$–0.8. Of the MW-like galaxies selected on the basis of their gas accretion history, we now select those with $M_{*,\mathrm{d}}/M_{*,\mathrm{tot}}$ values ∼0.7–0.8. In Fig. 11, we show the predicted [O/Fe]–[Fe/H] relation for all the MW galaxies selected on the basis of their accretion history (upper panel) and on the basis of the $M_{*,\mathrm{d}}/M_{*,\mathrm{tot}}$ ratio (lower panel), and the results are nearly the same. This result is robust against any morphological selection criterion we use to select MW-like galaxies.

In Fig. 12, we show the predicted cumulative stellar metallicity distribution (SMD) for our MW-like galaxy sample, compared to observations of solar neighbourhood stars from various authors. The predicted SMD has been computed by taking into account the SFHs of the galaxies whose assembled mass at $z \sim 2$ is greater than 75 per cent of their present mass. The predicted SMDs and the observations are normalized by requiring that the areas subtended by each curve have all the same values, equal to unity. The agreement between the observed and predicted SMD is remarkable. The position of the peak is much sensitive to the Type Ia SN normalization. With our assumption of $A_{\mathrm{Ia}} = 0.002$, the position of the peak of the SMD is satisfactorily reproduced. We also reproduce accurately the low-metallicity tail of the SMD, i.e. we predict the correct fraction of stars in the metallicity range [Fe/H] $\leq -0.7$. The high-metallicity tail, i.e. the number of stars with [Fe/H] $\geq 0.2$, is in reasonable agreement with the observations. It is worth to note that the assumption of the IMF may have some effect on the predicted SMD. Fe is produced mainly by Type Ia SNe, whose rate depends on the product of the parameters $k_\alpha$ and $A_{\mathrm{Ia}}$ of equation (6). $k_\alpha$ depends on the IMF, hence a change of the IMF would require a retuning of the parameter $A_{\mathrm{Ia}}$ in order to reproduce the correct present-day SN rate. However, it seems reasonable to assume that the quantity $k_\alpha$ $A_{\mathrm{Ia}}$ is constant and fixed in order to reproduce the present Type Ia SN remnant in MW-like galaxies. In this case, the IMF assumption is not relevant.

It may be interesting to compare our results with the ones obtained previously by other authors. A previous relevant theoretical study of the chemical evolution of spiral galaxies in a cosmological framework is the one of Nagashima & Okamoto (2006). In this paper, the authors find a good agreement between the predicted [O/Fe] versus [Fe/H] obtained for a sample of MW-like spiral galaxies and the observations of the abundances in local disc stars. These authors obtained also a good match between the predicted and the observed SMD. However, to model the Type Ia SN rate and Fe production, Nagashima & Okamoto (2006) considered a constant value for the delay time of the explosion, which seems rather unrealistic, as indicated by a large amount of observational and theoretical studies of the Type Ia SN rate in local and distant galaxies (Mannucci, Della Valle & Panagia 2006; Matteucci et al. 2006; Sullivan et al. 2006; Valiante et al. 2009) which, on the other hand, point towards continuous delay-time distributions for Type Ia SN explosions.

Other interesting results are those obtained by Colavitti et al. (2008). In this paper, the authors start from cosmological numerical CDM simulations and, from the merging history of the parent haloes, these authors infer the infall history of spiral galaxies, which is implemented in a numerical chemical evolution code and whose evolution is followed a posteriori. Colavitti et al. (2008) find an overall good agreement between their predicted abundances and the observational constraints. However, the merging histories are determined by means of simulations with a low time resolution. Furthermore, the assumption of a linear scaling between the baryonic accretion history and the CDM merging history may represent a raw approximation, as well as the fact that pure DM simulations permit to explore spatial scales of the order of $\sim$1 Mpc, considerably higher than the scales of a few kpc studied in the paper by Colavitti et al. (2008).

The one described in this section is the first attempt to reproduce the abundance ratios for such a wide set of chemical elements by means of a hierarchical SAM taking into account the lifetimes of LIMS and Type Ia SNe. Overall, from the various results discussed in this section, we find that most of the chemical evolution constraints considered here and concerning the MW galaxy are satisfactorily reproduced. We find that the results discussed in this section are very encouraging. The agreement between our predictions and the observations is remarkable, in particular concerning the [O/Fe]–[Fe/H] diagram and the SMD, given the very little fine-tuning of the parameters performed so far. For other elements shown in Fig. 5, better fits to the data could be achievable by means of a fine tuning of the adopted stellar yields, as is performed sometimes in theoretical studies of the chemical evolution of the solar neighbourhood (e.g. François et al. 2004).

### 3.2 Abundances in dwarf galaxies

In this section, we present our results concerning the chemical evolution of dwarf galaxies. In particular, we focus on the chemical abundances in dwarf spheroidal (dSph) galaxies, since for this kind of objects a large set of observational data is available from observations of the dSph in the Local Group. In this case, the selection on our galaxy catalogue is performed on the basis of the present stellar mass $M_*$, considering all the systems with $10^6 \leq M_*/\mathrm{M}_\odot \leq 5 \times 10^9$, broadly corresponding to the stellar mass range of local dwarf galaxies (Mateo 1998). In Fig. 13, we see the time evolution of the SFR for a few selected examples. One striking feature of Fig. 13 is the variety of the SFHs of the selected galaxies. For some systems

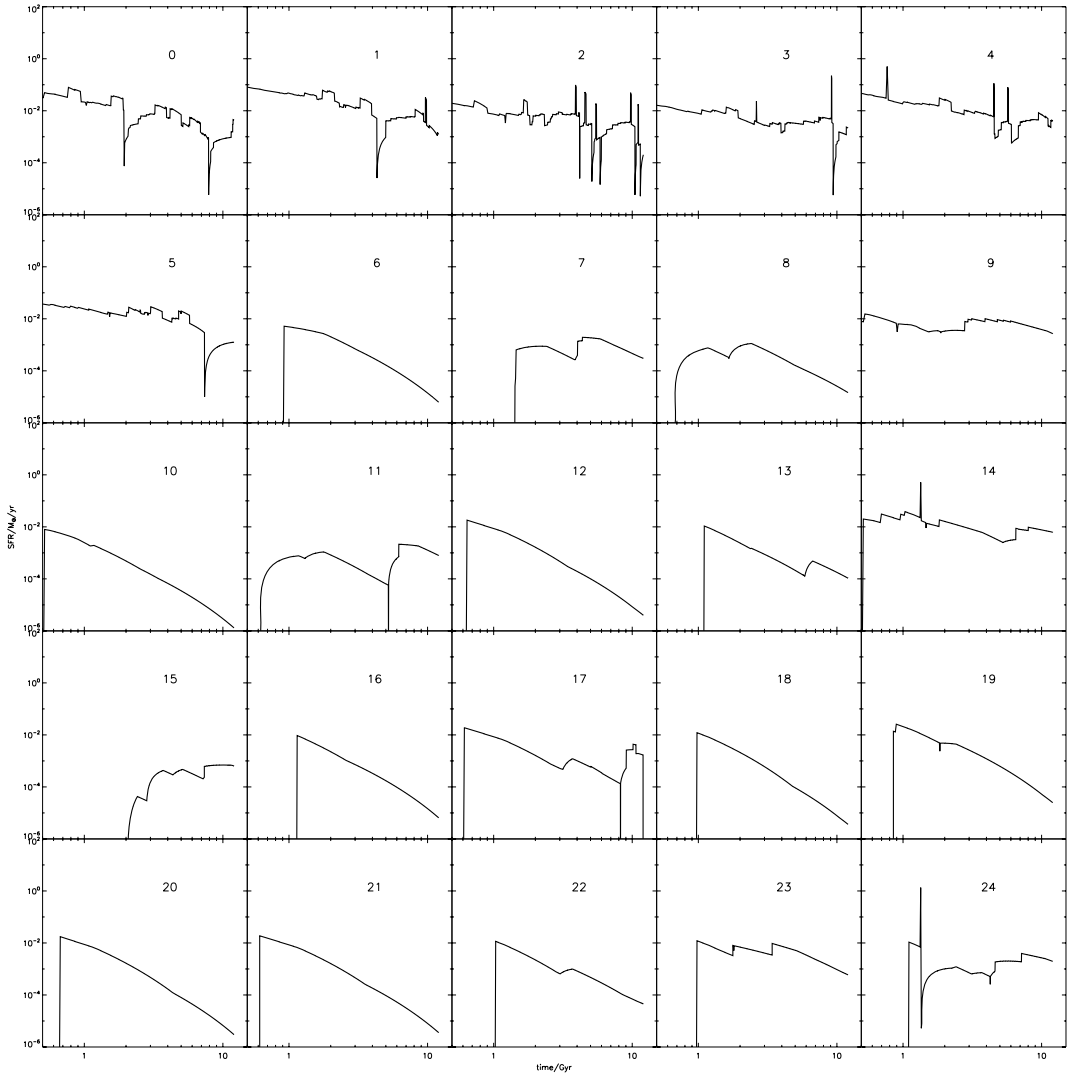


**Figure 13.** SFHs of a few dwarf galaxies selected according the criteria described in Section 3.2.

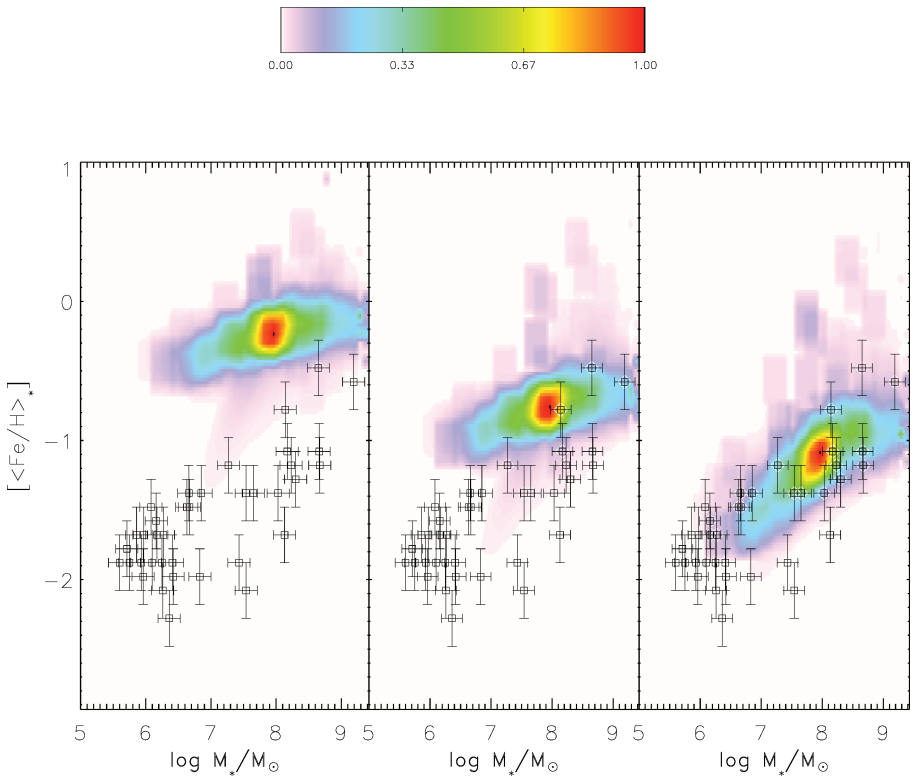


**Figure 14.** Predicted distribution of the average present-day stellar metallicity in dwarf galaxies versus present stellar mass. The colour code, shown by the bar at the top of the figure, represents the predicted number of galaxies with given $[\langle \mathrm{Fe/H} \rangle_*]$ with stellar mass $M_*$. The open squares with error bars are the observations in local dSphs, taken from Woo et al. (2008). In the left-hand panel, we assume that the chemical composition of the outflows $X_{i,\mathrm{out}}$ is the same as the one of ISM and $A_{\mathrm{Ia}} = 0.002$ as assumed for MW-like galaxies. In the central panel, we assume chemical compositions of the outflows as above and $A_{\mathrm{Ia}} = 0.0002$. In the right-hand panel, we assume $X_{i,\mathrm{out}} = \xi X_i$, with $\xi = 10$, and $A_{\mathrm{Ia}} = 0.0002$.

(e.g. the objects labelled 18 and 20 in Fig. 13), the SFH is maximum at the beginning, then smoothly and constantly decreasing. Some others have more than one peak (e.g. two, 11), mimicking the star-bursty behaviour of some real dSph galaxies, whose complex SFH is usually inferred from the observed colour–magnitude diagrams (CMDs; van den Bergh 1994; Hernandez, Gilmore & Valls-Gabaud 2000; Dolphin et al. 2005).

An important plot is the stellar metallicity versus stellar mass (Fig. 14), allowing us to test the SFHs of our dSphs and also to tune some fundamental parameters regarding their chemical evolution. In this figure, the stellar metallicity is represented by the average stellar Fe abundance $[\langle \mathrm{Fe/H} \rangle_*]$. This plot is of great interest since it is analogous to a mass–metallicity plot, with the difference that in general, in the mass–metallicity plots the stellar mass and the interstellar metallicities are represented, the latter usually derived by means of observations of O emission lines in brilliant H II regions of star-forming galaxies (Maiolino et al. 2008). Local dSphs are weakly star-forming systems and do not allow observations of emission lines in HII regions, however, a plot like such of Fig. 14 provides us with similar indications as a O/H versus $M_*$ plot, since $[\langle \mathrm{Fe/H} \rangle_*]$ is approximately

$$\langle \mathrm{Fe/H} \rangle_* \simeq \frac{\int (\mathrm{Fe/H})(t)\, \mathrm{d}M_*}{\int \mathrm{d}M_*} = \frac{\int (\mathrm{Fe/H})(t) \psi(t)\, \mathrm{d}t}{M_{*,\mathrm{tot}}}, \qquad (14)$$

i.e. the integral of the interstellar Fe abundance over the SFH (see Thomas, Greggio & Bender 1999). The predicted $[\langle \mathrm{Fe/H} \rangle_*]$–$M_*$ relation is compared to the one observed in local dwarf galaxies by Woo, Courteau & Dekel (2008). The observations indicate that the local dwarf galaxies clearly follow a mass–metallicity relation, i.e. that the smallest galaxies have the lowest metallicities, and that the stellar metallicity increases with stellar mass. In the left-hand panel of Fig. 14, we have assumed that dwarf galaxies can undergo mass loss under the same conditions as spiral galaxies, i.e. the chemical composition of the outflow is the same as the one of the ISM, $O_i(t) = X_i(t)\, O(t)$, and for the Type Ia SN realization probability the same value as assumed for spirals, $A_{\mathrm{Ia}} = 0.002$. In most of the cases, the model dwarf galaxies are considerably more metal rich than the observed ones. Furthermore, the predicted mass–metallicity relation is much flatter than the observational one. In the middle panel of Fig. 14, we show the predicted $[\langle \mathrm{Fe/H} \rangle_*]$–$M_*$ relation computed by assuming a chemical composition of the outflows as above and a very low value for the Type Ia SN realization probability, $A_{\mathrm{Ia}} = 0.0002$, i.e. one tenth of the value used for MW-like galaxies. This assumption certainly lowers the zero-point of the predicted mass–metallicity relation, however, does not affect its shape, which is still flatter than the observed one. Both the slope and the zero-point of the predicted mass–metallicity relation can be further improved by modifying our assumptions on metal loss in dwarf galaxies. In the right-hand panel of Fig. 14, we have assumed preferential loss of metals in the outflows, i.e. that for any chemical element different than H and He, the outflow rate in equation (2) is given by $\xi X_i(t)\, O(t)$, with $\xi = 10$, with $A_{\mathrm{Ia}} = 0.0002$. As can be seen, this assumption improves considerably the match between the predicted and observed mass–metallicity relation for dwarf galaxies. One first conclusion on chemical evolution of dwarf galaxies is that, in order to reproduce the slope of the observed mass–metallicity relation, one needs to assume that in dwarf galaxies mass loss must occur through metal-enhanced outflows. The

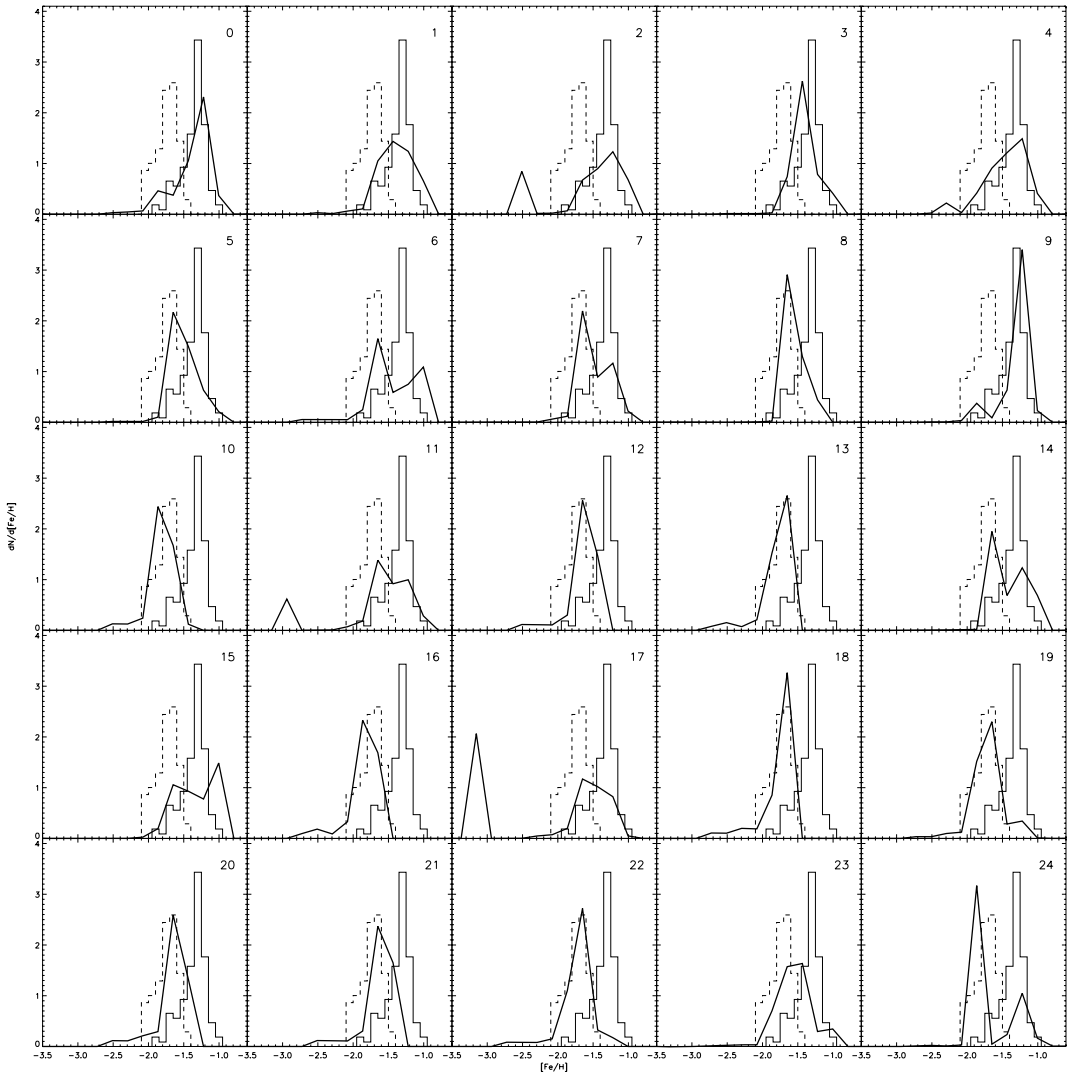


**Figure 15.** SMDs computed for the same set of dwarf galaxies presented in Fig. 13 (solid thick lines), compared with observational SMDs obtained for the Draco dSph (solid thin histograms) and for the Ursa Minor dSph (dashed thin histograms; see Bellazzini et al. 2002).

importance of mass loss in determining the mass–metallicity relation in dwarf galaxies has already been ascertained (Dekel & Silk 1986). The fundamental role played by metal-enhanced outflows has already been discussed by some previous investigations on the mass–metallicity and luminosity–metallicity relations in dwarf galaxies by means of semi-analytic galaxy formation models (Somerville & Primack 1999). All the following results presented in the remainder of this section are computed by assuming metal-enhanced outflows in dwarf galaxies. A more detailed discussion on the origin and importance of metal-enhanced outflows in dwarf galaxies will be presented in Section 4.

It may be interesting to see the effects of the SFHs shown in Fig. 13 on the metallicities of the stellar populations of dwarf galaxies. In the remainder of this section, we will compare our predictions with observational data regarding local dSph galaxies, whose stellar masses are in general of the order of $10^8\,\mathrm{M}_\odot$ or lower (Mateo 1998). For this reason, from this point on, in our analysis we will consider only the model galaxies with present stellar masses $M_* \leq 10^8\,\mathrm{M}_\odot$. In Fig. 15, we can see the predicted SMDs for the same objects as those presented in Fig. 13. In this figure, for comparison we plot also the SMDs observed in two local dSphs, i.e. Draco and Ursa Minor. The predicted SMDs have been computed with a number of bins comparable with the ones of the data of Bellazzini et al. (2002), which have 12–20 bins. For most of the model galaxies presented in Fig. 15, one dominant peak is recognizable, which corresponds to a dominant metallicity of the stellar populations of the dwarf galaxies. Some objects present two unresolved peaks (e.g. 6, 14), whereas others have two clearly distinct peaks at different metallicity values (e.g. 11, 17). All the model galaxies with a single-peaked SMD or with two very close, non-resolved peaks have in general smooth SFHs, or presenting small oscillations, or a few very short prominent peaks in their SFH. All the systems presenting two resolved peaks in the SMD have in general bursty SFHs, characterized by quite broad and distinct peaks (e.g. 11, 17), or frequent short and high peaks overimposed to an overall continuous SFH (e.g. 2). It is worth to note that in most of the cases, the positions of the peaks of the predicted SMDs agree with the ones of the observed SMDs. It is also worth to note that the lowest metallicities which can be probed by our analysis depend on the SF history. In Section 3.1, we have seen that in MW-like galaxies, we could not explore the metallicity region [Fe/H] $< -2.5$. MW-like galaxies have strong SF histories, hence a metallicity [Fe/H] $\sim -2.5$ can be reached in a time shorter

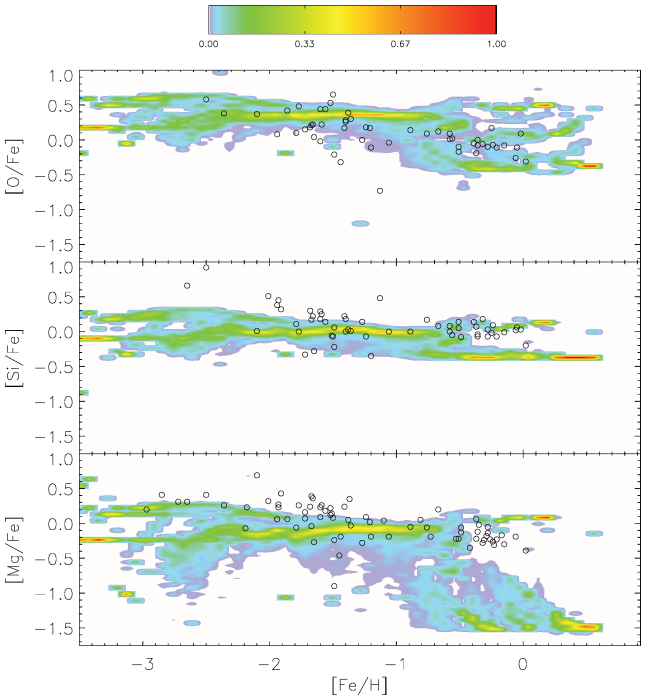


**Figure 16.** Predicted distribution of the abundance ratios [X/Fe] versus [Fe/H] for dSph galaxies. The colour code, shown by the bar at the top of the figure, represents the predicted number of stellar populations belonging to dwarf galaxies with a given abundance ratio at metallicity [Fe/H], normalized to the total number of stellar populations with that metallicity. The observational data (open circles) are observations in local dSphs taken from a compilation by Lanfranchi & Matteucci (2003).

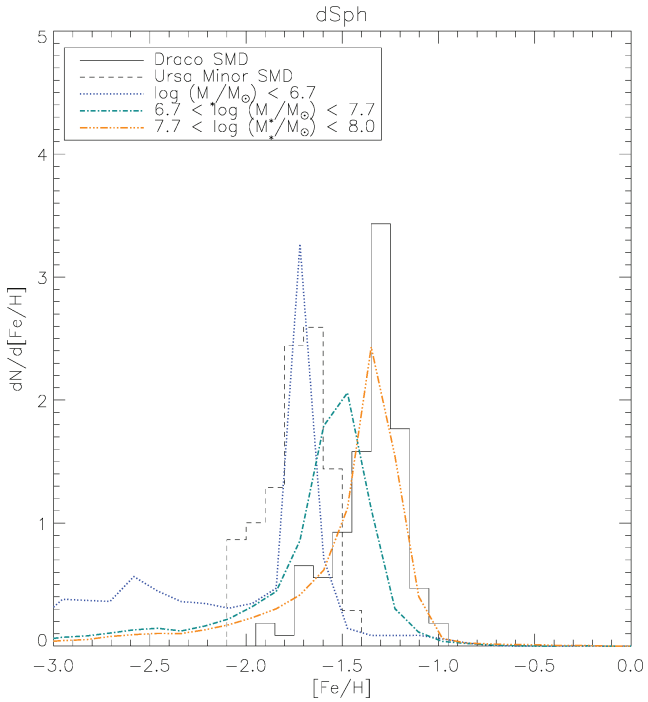


**Figure 17.** Predicted cumulative SMD of selected dwarf galaxies belonging to three different mass bins (solid thick lines) compared with observational SMDs obtained for the Draco dSph (solid histogram) and for the Ursa Minor dSph (dashed histograms).

than the time-step used in our model. On the other hand, for dwarf galaxies, characterized by lower SF rates, the lowest metallicity probed is [Fe/H] $<-3.5$, reached sometimes on time-scales higher than our time-step. Another reason for the low metallicities is the adopted value for $A_{\rm Ia}$, which in the case of dwarfs is one tenth of the value assumed for MW-like galaxies.

Furthermore, in this case, owing to the large set of chemical elements studied here, we are able to produce predictions for the abundance ratios of several chemical elements. In Fig. 16, we show our predictions for the [O/Fe] versus [Fe/H], [Si/Fe] versus [Fe/H] and [Mg/Fe] versus [Fe/H]. For these elements, the abundances are measurable in single stars of local dSphs. The predictions represent the abundance ratios of the stellar populations belonging to the selected galaxies, as described in Section 3.1. From Fig. 16, we can see how, for any element considered here, the characteristic decreasing trend of [$\alpha$/Fe] versus [Fe/H] is successfully reproduced. In our models, this trend is due to the delay between Type II SNe explosions and Type Ia SN explosions, as in classical chemical evolution models taking into account enrichment from Type Ia and Type II SNe (Matteucci 2001 and references therein).

While in the [O/Fe] versus [Fe/H] plot the observed data overlap with our predictions, in the other two plots the measured [$\alpha$/Fe] are often underestimated, in particular for [Fe/H] $> -1$. The same discrepancy was found also when discussing the results for MW-like galaxies, and is due to the adopted stellar yields of Woosley & Weaver (1995), which lead the models to underestimate the [Mg/Fe] and [Si/Fe] also in the solar neighbourhood (François et al. 2004). In these plots, a fine-tuning of the stellar yields as a function of the initial stellar mass would be required to reproduce the observations. Furthermore, we see that our models for dwarf galaxies predict a wider [Fe/H] range than the one spanned by the observational data, but this plot is not useful to understand the relative fractions of the stellar populations of various metallicities. More useful in this regard is Fig. 17, where we show the predicted cumulative SMD of all the dwarf galaxies, divided in three stellar mass bins (see legend of Fig. 17), compared to the observational SMDs of the Draco and Ursa Minor dSph. The predicted SMDs are computed by taking into account all the stellar populations of any selected galaxy falling in each mass bin. The cumulative SMDs computed for various mass bins are in very good agreement with the observed ones, at least concerning the positions of the peaks. In each mass bin, the predicted SMDs span very broad metallicity ranges. In particular, in this case we predict the existence of stars at very low metallicities, [Fe/H] $\leq -2$. By integrating the quantity d$N$/d[Fe/H] over different metallicity ranges, it is possible to estimate the relative fractions of the stellar populations at various metallicities. For the objects in the lowest mass bin, no stellar population presents [Fe/H] $> -0.7$. For the objects in the intermediate and highest mass bins, a very small fraction lower than 1 per cent have stellar populations with [Fe/H] $> 0$.

Finally, it is interesting to note that we predict the substantial presence of very low metallicity stars with [Fe/H] $< -2$, with percentages of $\sim$40, $\sim$15 and $\sim$10 per cent in the lowest, intermediate and highest mass bin, respectively.

Relevant previous studies of the chemical evolution of dSphs are those of Lanfranchi, Matteucci & Cescutti (2006). Even if not carried by means of an *ab initio* galaxy formation model, but by means of galactic chemical evolution models whose SFHs are tuned from constraints of CMD observations (see Calura, Lanfranchi & Matteucci 2008b), these works are useful since they allow to have some constraints on the parameters affecting this kind of analysis. In particular, Lanfranchi & Matteucci (2007) present the effects of

the wind efficiency on the predicted SMDs of dSphs, showing how a model where the galactic wind is suppressed leads to too metal-rich stellar populations. The results of Lanfranchi & Matteucci (2004, 2007) suggest that a strong wind efficiency is necessary to reproduce the abundance ratios and the SMDs of dwarf galaxies.

A previous study of the chemical evolution of dwarf galaxies within a cosmological framework is the one of Salvadori, Ferrara & Schneider (2008). These authors model chemical evolution of dwarf galaxies by taking into account the stellar lifetimes of LIMS and of massive stars, however, they do not consider Type Ia SN explosions. Salvadori et al. (2007) explain the observed decline of [$\alpha$/Fe] versus [Fe/H] in local dSphs by means of differential galactic winds. This result is apparently in contrast with a large variety of chemical evolution studies, which underline the importance of the time delay of Type Ia SN explosions in explaining the decrease of the [$\alpha$/Fe] versus [Fe/H] in local dSphs (Recchi, Matteucci & D'Ercole 2001; Ikuta & Arimoto 2002; Lanfranchi & Matteucci 2003; Lanfranchi, Matteucci & Cescutti 2006; Recchi et al. 2006; Marcolini et al. 2008).

Very recently, Sawala, Scannapieco & White (2009) studied the chemical evolution of local dwarfs in a cosmological framework by means of high-resolution hydrodynamical numerical simulation, including also Type Ia and Type II SN enrichment. Their results indicate that the chemical properties of dwarf galaxies are driven by several aspects, such as the SN feedback, the ultraviolet (UV) background and their gravitational potential. Their results stress the importance of efficient metal-enhanced outflows, fundamental for reproducing the stellar mass–metallicity relation.

A numerical study of the SMDs of dSphs has been performed by Ripamonti et al. (2007). Their results point towards the substantial presence of very low metallicity [Fe/H] $< -3$ stars in dSphs, in agreement with the results found in this paper. If no observational bias against these stars is present, possible solutions to this problem invoke a primordial IMF truncated for stellar masses below 1 $M_\odot$ or a pre-enrichment of the gas. However, very recently, the presence of extremely low metallicity stars has been detected in ultrafaint dwarf galaxies (Frebel et al. 2009).

### 3.3 Abundances in elliptical galaxies

We conclude this section presenting our chemical evolution results obtained for elliptical galaxies. Elliptical galaxies are selected on the basis of their present-day $(B - V)$ colour. In specific, we consider elliptical galaxies all the systems with present $(B - V) \geq 0.85$, following Roberts & Haynes (1994). We perform a further cut on the basis of the present-day velocity dispersion $\sigma$, considering all the systems with $30 \leq \log(\sigma/\mathrm{km\,s^{-1}})$. This range for the velocity dispersion is similar to the one spanned by the observational data of Thomas et al. (2005), who determined observationally the integrated stellar chemical abundances in a sample of local field ellipticals, and whose set of data will be used here for comparison with our predictions. In Fig. 18, we show the SFHs of a few ellipticals selected according to the criteria described above. The numbers present in each panel of Fig. 18 indicate the present-day stellar masses of the selected galaxies. The selected SFRs are characterized by numerous peaks occurring in most of the cases at cosmic times $\leq$6 Gyr, corresponding to redshift $z > 1$. In general, galaxies with larger stellar masses exhibit higher SFR values. The SFHs of the objects shown in Fig. 18, with little or no substantial SF in the last few Gyr, are qualitatively in agreement with the SFHs of early-type galaxies drawn from other SAMs (De Lucia et al. 2006; Pipino et al. 2008).

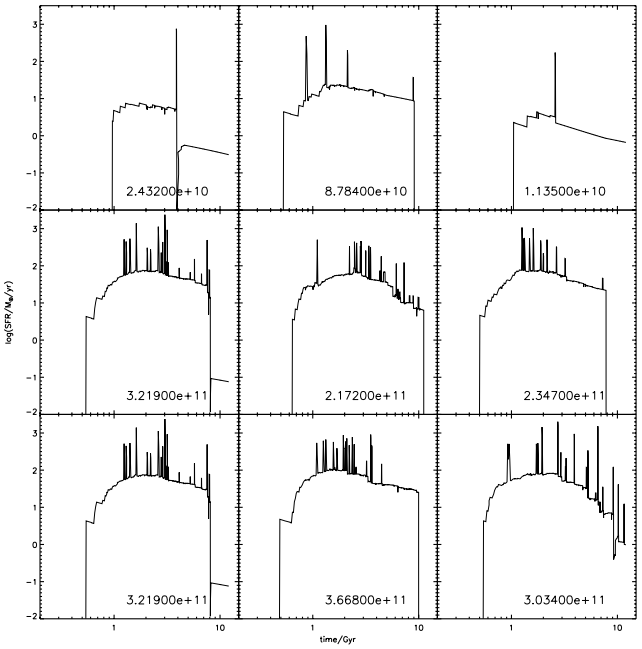


**Figure 18.** SFHs of a few elliptical selected according the criteria described in Section 3.3.

Generally, in local ellipticals the stellar abundances are measured by means of absorption-line indices, such as Mg $b$ and $\langle \mathrm{Fe} \rangle = 0.5$ (Fe 52720 + Fe 5335) (see Thomas et al. 2005 and references therein). This means that the observational abundances are luminosity-averaged values, which in principle represent underestimates to the true, mass-averaged abundances, which are the ones computed by means of our models, because of the fact that at constant age, metal-poor stars are brighter (Greggio 1997). However, as discussed in several papers (Matteucci, Ponzone & Gibson 1998; Thomas, Greggio & Bender 1999; Recchi, Calura & Kroupa 2009), detailed chemical evolution calculations show that the difference between mass-averaged and luminosity-averaged abundances is very small, typically of the order of a few 0.01 dex. This result is not dependent on fundamental chemical evolution parameters, such as the stellar IMF (Recchi et al. 2009). For this reason, we neglect this difference and we compare our predicted mass-averaged stellar abundances to the ones derived observationally by means of absorption-line indices.

In the upper panel of Fig. 19, we show the predicted average stellar $\alpha$/Fe ratio versus velocity dispersion, computed assuming a Salpeter IMF and compared with a set of local observations by Thomas et al. (2005). In this case, the predicted $[\langle \alpha/\mathrm{Fe} \rangle_*]$ is computed considering O as representative of $\alpha$ elements. To compute our predictions, in Fig. 19 we use a standard Salpeter IMF, and a Type Ia SN realization probability $A_{\mathrm{Ia}} = 0.002$. As we will see later, with our standard assumptions, this value allows us to correctly reproduce the zero-point of the stellar [$\alpha$/Fe]–$\sigma$ relation.

While the observations indicate a positive correlation between [$\alpha$/Fe] and $\sigma$, with galaxies with larger $\sigma$ presenting larger $\alpha$ enhancement, our predictions indicate a flat [$\alpha$/Fe]–$\sigma$ relation. In general, the observed [$\alpha$/Fe]–$\sigma$ is interpreted in terms of smaller formation time-scales in larger ellipticals, in which the chemical enrichment is dominated by the contribution of Type II SNe, hence most of the stars form with a chemical composition rich of $\alpha$ elements (Matteucci 1994; Thomas et al. 2005). On the other hand, smaller galaxies present lower stellar [$\alpha$/Fe] since they form on

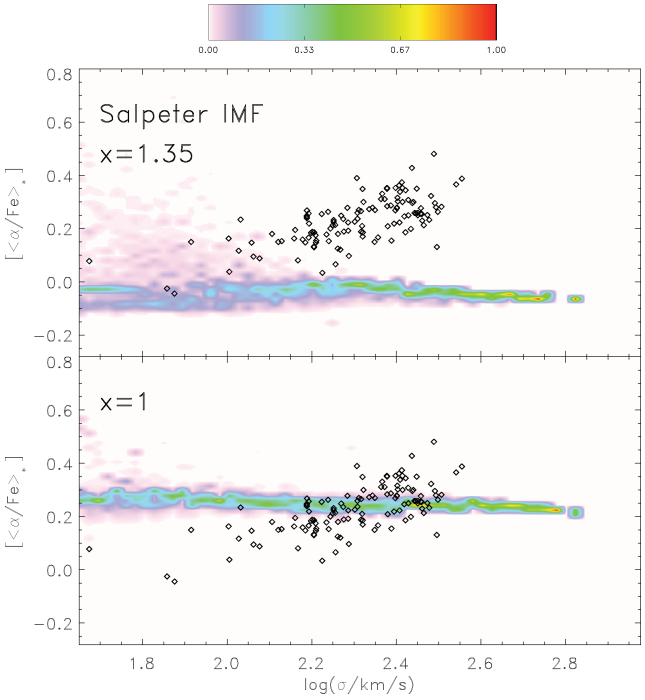


**Figure 19.** Predicted stellar average $\alpha$/Fe ratio versus velocity dispersion compared to local observations by Thomas et al. (2005) (open diamonds). The colour code, shown by the bar at the top of the figure, represents the predicted number of galaxies with given $[\langle\alpha/\mathrm{Fe}\rangle_*]$ with velocity dispersion $\sigma$, normalized to the total number of galaxies with that $\sigma$. In the upper panel, we show our results computed with a Salpeter IMF whereas in the lower panel we have assumed an IMF slope of $x = 1$.

longer time-scales, comparable to the exploding times of Type Ia SNe, whose contribution to the Fe enrichment of the ISM is relevant, lowering the average stellar [$\alpha$/Fe]. Matteucci (1994) has shown that a monolithical galaxy formation scenario for ellipticals is successful in reproducing the observed stellar abundance ratios. According to this scenario, in ellipticals SF stops owing to the onset of galactic winds, which develop on smaller time-scales in larger ellipticals, according to an inverse-wind scheme. Calura et al. (2008a) have confirmed that gas outflows should occur on smaller time-scales in large galaxies, according to a 'downsizing' pattern for galaxy formation.

The impossibility to reproduce the observed [$\alpha$/Fe]–$\sigma$ relation is a well-known problem, common to many hierarchical SAM. The reason is that, in hierarchical models, the SF of large elliptical galaxies is extended until relatively recent times, hence without avoiding that large amounts of Fe are restored by Type Ia SNe into the ISM while SF is still active. In general, this leads large galaxies to present lower average stellar [$\alpha$/Fe], i.e. to an anticorrelation between [$\alpha$/Fe] and $\sigma$ (Thomas 1999; Nagashima et al. 2005; Pipino et al. 2008), contrary to what the observations indicate. On the other hand, by assuming a simple Salpeter IMF constant in time, our results indicate rather a flat relation between these two quantities. This is still at variance with the observations, however, this should be certainly regarded as a an improvement with respect to the previous attempts discussed above.

Our basic assumptions, i.e. a Salpeter IMF, the inclusion of interaction-triggered starbursts and AGN feedback do not allow us to produce a positive correlation between the stellar [$\alpha$/Fe] and $\sigma$. In a recent paper, Arrigoni et al. (2009) studied the chemical evolution of local ellipticals by means of a SAM for galaxy formation which includes AGN feedback. Their main result concerns the capability to reproduce the observed correlation between stellar [$\alpha$/Fe] and stellar mass, after a fine-tuning of the Type Ia SN constant and by assuming an IMF slope $x = 1.1$, where the canonical Salpeter slope is $x = 1.35$. As already stressed, in chemical evolution studies the Type Ia SN constant $A_{\mathrm{Ia}}$ is an uncertain parameter, however, the IMF is in general better constrained by local observations. Now we aim at studying the [$\alpha$/Fe]–$\sigma$ relation in the same conditions as the ones of Arrigoni et al. (2009), i.e. assuming a flatter IMF. In the lower panel of Fig. 19, we show the stellar [$\alpha$/Fe]–$\sigma$ relation predicted for massive galaxies, obtained by considering a constant IMF with index $x = 1$. This figure shows clearly that the assumption of a constant IMF flatter than the Salpeter has the effect of lifting the zero-point of the predicted [$\alpha$/Fe]–$\sigma$ relation, but has no effect on its slope. This is also in agreement with the discussion about the role of the IMF in the chemical evolution of early-type galaxies of Pipino et al. (2008).

Recent observational and theoretical results seem to indicate a dependency between the SFR and the slope and the upper mass limit of the IMF. In normal SF conditions, i.e. in local regions with SFRs $< 100\,\mathrm{M}_\odot\,\mathrm{yr}^{-1}$, a standard IMF slope $x \sim 1.3$ for stellar masses $> 1\,\mathrm{M}_\odot$ is commonly accepted (Kroupa 2002; Recchi et al. 2009). On the other hand, in local starbursts, in the cores of stellar clusters and in ultracompact galaxies, with SFRs $> 100\,\mathrm{M}_\odot\,\mathrm{yr}^{-1}$, various results indicate a flatter IMF, with a slope $x \leq 1$ (Dabringhausen, Kroupa & Baumgardt 2009; Elmegreen 2009). Further evidences in favour of a flat IMF in environments undergoing strong SF come from chemical evolution models, which, in order to be able to explain the oversolar [$\alpha$/Fe] values observed in the hot intracluster gas, must necessarily invoke an IMF skewed towards massive stars (Gibson & Matteucci 1997; Portinari et al. 2004). Motivated by these results, now we aim at investigating the impact of a SF-dependent IMF on the stellar [$\alpha$/Fe] versus $\sigma$ relation predicted by local ellipticals. Our aim is also to test how our results depend on other ingredients of the SAM model used in this paper, such as interaction-triggered starburst in massive galaxies and AGN feedback, and the importance of including or neglecting these effects in conjunction with the main chemical evolution parameter, i.e. the IMF.

In the left-hand panel of Fig. 20, we show the predicted [$\alpha$/Fe]–$\sigma$ relation obtained by considering a SF-dependent IMF, characterized by a standard Salpeter slope ($x = 1.35$) in objects with SFRs $< 100\,\mathrm{M}_\odot\,\mathrm{yr}^{-1}$, and $x = 1$ in objects with SFRs $> 100\,\mathrm{M}_\odot\,\mathrm{yr}^{-1}$. This assumption in consistent with the study of Dabringhausen et al. (2009), indicating IMF slopes $x \leq 0.7$ in starburst and ultracompact galaxies, with SFRs of 10–$100\,\mathrm{M}_\odot\,\mathrm{yr}^{-1}$. Here we consider an IMF slope $x = 1$, close to the upper limit of Dabringhausen et al. (2009), since this does not require substantial modifications of the parameters of our SAM to reproduce the main local observational constraints, such as the luminosity function or the Tully–Fisher relation. In this case, we see that the use of this IMF allows us to considerably improve our results, reproducing the observed correlation between [$\alpha$/Fe]–$\sigma$ and bringing our results in good agreement with the observations on a large range of velocity dispersions. In the right-hand panel of Fig. 20, we show our results obtained with a model which does not include encounter-triggered starbursts, but it does include a SF-varying IMF as described above. In this case, the predicted [$\alpha$/Fe]–$\sigma$ relation is too shallow to reproduce the observations. This result outlines the importance of interaction-driven starbursts in determining the [$\alpha$/Fe]–$\sigma$ relation of local ellipticals. At this stage, it may be interesting to test also the role of the AGN feedback in the chemical evolution of ellipticals. In Fig. 21, we compare our results obtained with our standard model

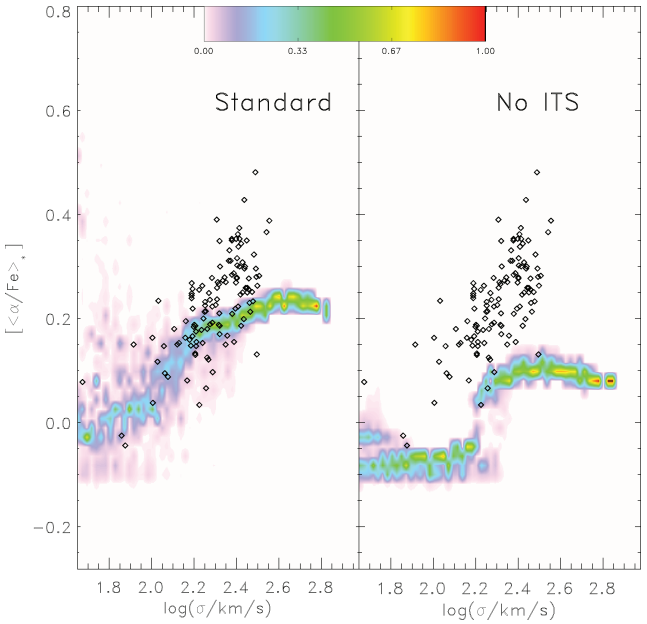


**Figure 20.** Predicted stellar average $\alpha$/Fe ratio versus velocity dispersion, compared to local observations by Thomas et al. (2005, open diamonds). The colour code represents the predictions, as described in Fig. 19. In the left-hand panel, our results have been computed by means of a SF-dependent IMF and our standard assumptions, which include starburst-triggered interactions at high redshifts and AGN feedback. In the right-hand panel, we have assumed a SF-dependent IMF and AGN feedback but we have suppressed starburst-triggered interactions.

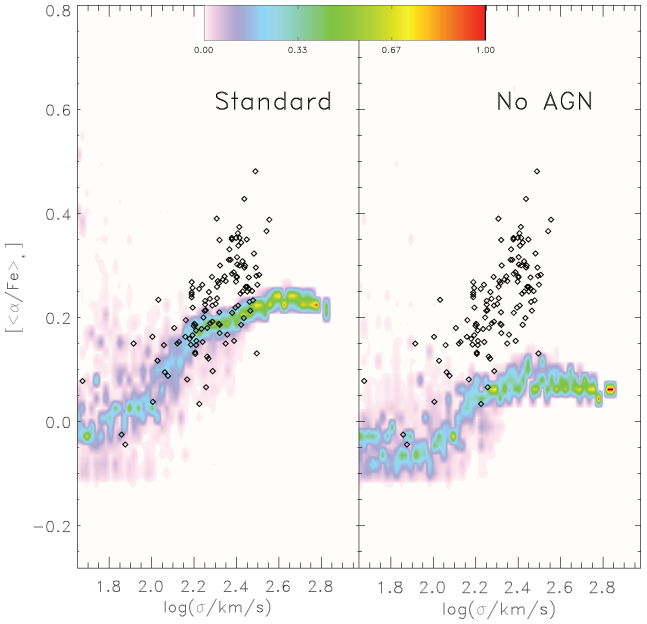


**Figure 21.** Predicted stellar average $\alpha$/Fe ratio versus velocity dispersion, compared to local observations by Thomas et al. (2005, open diamonds). The colour code represents the predictions, as described in Fig. 19. In the left-hand panel, our results have been computed by means of a SF-dependent IMF and our standard assumptions, which include starburst-triggered interactions at high redshifts and AGN feedback. In the right-hand panel, we have assumed a SF-dependent IMF and starburst-triggered interactions but we have suppressed the effect of AGN feedback.

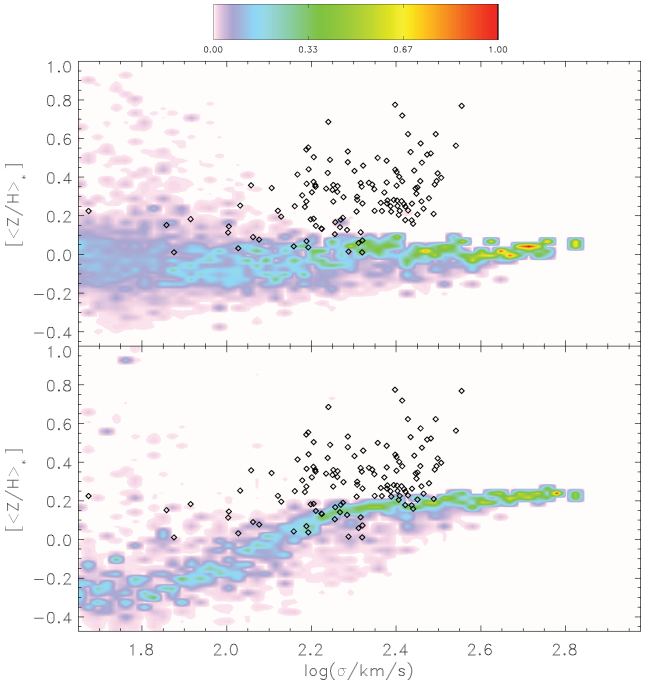


**Figure 22.** Predicted stellar average $Z$/H versus velocity dispersion $\sigma$, compared to local observations by Thomas et al. (2005, open diamonds). In the upper and lower panels, we show the results obtained by assuming a Salpeter IMF and a SF-dependent IMF (i.e. with $x = 1.35$ for systems with SFR $\leq 100\,M_\odot\,yr^{-1}$ and with $x = 1$ for systems with SFR $\leq 100\,M_\odot\,yr^{-1}$), respectively. The colour code, shown by the bar at the top of the figure, represents the predicted number of galaxies with given $[\langle Z/H\rangle_*]$ with velocity dispersion $\sigma$, normalized to the total number of galaxies at the considered $\sigma$.

and with a SF-dependent IMF with the ones achieved with a model which does include interaction-triggered starbursts, but which does not take into account the effect of AGN feedback in massive galaxies. The model with no AGN feedback has a shallower slope than the standard model and produces a poor match to the observations. This indicates that also the AGN feedback must play some important role in shaping the [$\alpha$/Fe]–$\sigma$ relation of local ellipticals.

In summary, in order to reproduce the correlation between the stellar [$\alpha$/Fe] and $\sigma$ of local ellipticals with our SAM, three basic ingredients seem to be required: (i) encounter-triggered starbursts at high redshift; (ii) AGN feedback; (iii) a SF-dependent IMF, flatter than the Salpeter in systems with strong SF. It is worth to note how a small decrease of the IMF slope allows us to considerably improve our results. A further decrease of the IMF index $x$ may possibly improve our results, but, in order to reproduce the local constraints, it would probably require a recalibration of the main parameters of the SAM to reproduce the local constraints. This will be the subject of future work.

The predicted mass–stellar metallicity relation is shown in Fig. 22, compared to the same relation as observed in local ellipticals (Thomas et al. 2005). In the upper panel of Fig. 22, we present our results obtained with a Salpeter IMF. In this case, we predict a basically flat $[\langle Z/H\rangle_*]$ versus $\sigma$ relation, whereas the data indicate a positive correlation between these two quantities. In the lower panel of Fig. 22, the $[\langle Z/H\rangle_*]$–$\sigma$ relation is computed by assuming a SF-dependent IMF as described above. Again, this assumption improves considerably our fit to the observational data. This plot provides a further, independent indication that the assumption of

a SF-dependent IMF is a possible solution to the long-standing problem of explaining the chemical abundances in ellipticals with hierarchical SAMs.

When comparing our predictions with observations, it is worth to stress that the observational $[\langle Z/\mathrm{H}\rangle_*]$ versus $\sigma$ is likely affected by a template bias (Proctor et al. 2004; Nagashima et al. 2005; Thomas et al. 2005), which reflects the fact that the stellar population models used to determine the metallicities are based on stellar spectra in which some stars present a subsolar [$\alpha$/Fe]. This effect could cause a steep $[\langle Z/\mathrm{H}\rangle_*]$ versus $\sigma$ relation, but, as shown by Thomas et al. (2005), it leaves basically unchanged the $[\langle \alpha/\mathrm{Fe}\rangle_*]$ versus $\sigma$ relation. Furthermore, as outlined by Pipino et al. (2008), the fact that elliptical galaxies exhibit strong metallicity gradients makes a detailed comparison between our predicted $[\langle Z/\mathrm{H}\rangle_*]$ versus $\sigma$ relation with observations quite difficult, and is likely to mimic a steeper $[\langle Z/\mathrm{H}\rangle_*]$ versus $\sigma$ relation, leaving essentially unchanged the $[\langle \alpha/\mathrm{Fe}\rangle_*]$ versus $\sigma$.

Finally, it is important to stress that in this paper, to compute the integrated stellar abundances in early-type galaxies, we have considered the integral SF histories of our selected galaxies, represented by the sum at each time-step of the SF histories of all the progenitors. As stressed by Pipino et al. (2008), the most massive progenitors have in general shorter SF time-scales and should dominate the integrated stellar abundances. For some systems, this may cause an underestimation of the stellar [$\alpha$/Fe] ratios by 0.1–0.2 dex. This effect is not taken into account at the present time, as considering in detail the SFHs of the single progenitors for all our galaxies would require considerable computational times. A subsequent paper completely dedicated to this aspect is currently under preparation.

## 4 DISCUSSION AND CONCLUSIONS

The major aim of the present paper is to model chemical evolution by means of a hierarchical SAM by taking into account properly all the various stellar sources. We also aim at providing chemical evolution predictions computed by means of SF and infall histories derived from first principles, by means of an *ab initio* approach. Beside high-mass stars, dying as core-collapse Type II SNe, we consider also the contributions from Type Ia SNe and LIMS. A continuous delay-time distribution is assumed for Type Ia SNe, relevant producers of some important elements, such as Fe and Si. We also consider finite lifetimes for LIMS, which are important producers of C and N. Our methods allow us to provide, for the first time, chemical evolution predictions for a large set of chemical elements, produced by stars of various types on different time-scales. This is particularly useful to study the abundance ratios between elements synthesized by different stellar sources on various time-scales, which are helpful tools to measure the time-scales of SF in galaxies of various masses and morphologies. We studied chemical evolution in various galactic types, comparing our predictions with available observations of chemical abundances in the MW, in local dwarf galaxies and in local ellipticals.

First, we studied the abundance ratios versus metallicity for MW-like galaxies. We compared our predictions to observations available for local stars of the solar neighbourhood for various elements. Overall, concerning the most important constraints, we found a good agreement between our predictions and the observations. In the [O/Fe] versus [Fe/H] plot, our results for MW-like galaxies indicate the presence of a horizontal population of stars with metallicity $-2 \leq$ [Fe/H] $\leq -0.2$ and constant [O/Fe] $\sim -0.2$ to $-0.3$. This population is the result of substantial late infall episodes of pristine gas, very frequent in the selected MW-like galaxies, which have the effect of decreasing the metallicity of the most recently formed stellar populations, leaving unchanged their [O/Fe] ratio. When we consider only the galaxies with at least 75 per cent of the present-day mass already assembled at $z = 2$, this horizontal population of stars with constant [O/Fe] $\sim -0.3$ disappears. These galaxies do not experience major accretion episodes at epochs after $\sim$6 Gyr. If we consider only this subset of galaxies, the observational [O/Fe]–[Fe/H] is accounted for. Our results concerning the [O/Fe] versus [Fe/H] plots exclude that our Galaxy experienced major gas accretion episodes within the last few Gyr, either due to merging with gas-rich, low-metallicity dwarf galaxies, or due to infall of pristine gas. This is in agreement with a large set of previous results based on the interpretation of abundances observed in MW disc and halo stellar populations and on kinematical studies of the various components of the MW (e.g. Gilmore et al. 2002; Colavitti et al. 2008 and references therein).

The typical decrease of the observed [$\alpha$/Fe] versus [Fe/H] plot is reproduced, as well as the observed trends for the other abundance ratios versus [Fe/H]. However, for other elements, the predictions are shifted downwards with respect to the observed abundance ratios. This is due to the adopted stellar yields, which in most cases lead to underestimating the observed abundance pattern. For elements other than O, the uncertainty in the stellar yield is a well-known problem of chemical evolution models of the solar neighbourhood (François et al. 2004). Furthermore, the IMF is likely to play some effects on the [X/Fe] versus [Fe/H] plots. For instance, with a Salpeter IMF, we predict an anticorrelation between [C/Fe] and [Fe/H], whereas the observational data indicate a substantially flat behaviour. We have shown how, by assuming the IMF of Kroupa et al. (1993) and by slightly modifying the stellar yields of C for both intermediate mass and massive stars, it is possible to improve our fit to the [C/Fe]–[Fe] diagram. From the study of the local SMD, we showed that we can correctly reproduce the position of the peak and the low-metallicity tail of the observed SMD. Also the predicted fraction of stars with metallicities $0 \leq$ [Fe/H] $\leq +0.2$ is in reasonable agreement with the observational data.

By assuming that the chemical composition of the outflows is the same as the one of the ISM and the same value for Type Ia SN realization probability $A_{\mathrm{Ia}}$ as assumed for MW-like galaxies, we severely overestimate the stellar metallicities of dwarf galaxies. Differential outflows, where metals are lost more efficiently than H and He, have a major effect on the slope of the predicted $\langle[\mathrm{Fe/H}]\rangle_*$–$M_*$ relation, whereas the quantity $A_{\mathrm{Ia}}$ affects primarily the zero-point of this relation. The assumptions of strongly enhanced outflows and of a lower value for $A_{\mathrm{Ia}}$ substantially decrease the average stellar metallicity of dwarf galaxies, yielding a better match between predictions and observations in the $\langle[\mathrm{Fe/H}]\rangle_*$–$M_*$ diagram. Other theoretical results outline the role of metal-enhanced outflows in dwarf galaxies (see Recchi et al. 2008). The physical justification for differential mass loss from dwarf galaxies has been studied in the past by means of numerical simulations. Mac Low & Ferrara (1999) modelled the effects of SN explosions in dwarf galaxies, finding that the metal ejection is much more efficient in lower mass galaxies. By means of two-dimensional (2D) hydrodynamical simulations, D'Ercole & Brighenti (1999) studied the feedback of a starburst on the ISM of typical gas-rich dwarf galaxies. They showed that metals are expelled more easily than the global ISM since the metal-rich material shed by the massive stars belongs to a very hot phase of the ISM, which can be easily accelerated to velocities higher than the escape speed and leave the galaxy. On the other hand, the interstellar gas, heated up by the SN explosions is only temporarily affected

by the starburst, and the galaxy is able to recover a cold ISM after a time of the order of $\sim$100 Myr from the starburst. Furthermore, results from chemical evolution models suggest that heavy elements should be lost more effectively than H to reproduce the global properties of dwarf galaxies (Pilyugin 1993; Marconi, Matteucci & Tosi 1994). The existence of metal-enhanced outflows from star-forming galaxies has also been recently confirmed by observations of local starbursts (Martin, Kobulnicky & Heckman 2002; Ott, Walter & Brinks 2005).

Our results concerning the abundance ratios of dwarf galaxies are compared to the abundances observed in local dSphs. Also in this case, the characteristic decreasing trend of [$\alpha$/Fe] versus [Fe/H] is reproduced, and explained as due to the delay between Type II SNe explosions and Type Ia SN explosions.

The study of the individual and cumulative SMDs of dwarf galaxies of various masses provides a satisfactory agreement between predictions and observations. Furthermore, this result is a direct consequence of having assumed metal enhanced outflows in dwarf galaxies and a low value for $A_{\rm Ia}$. The only discrepancy concerns the fraction of stars with metallicity [Fe/H] $\leq -2$. Our predictions indicate that they must be present in substantial fractions, in particular in galaxies with the lowest masses. The observational SMDs used in this paper do not indicate the presence of these low metallicity stars in dSphs. However, very recently a few extremely low metallicity stars have been detected in the Sextans and Draco dSphs and in ultrafaint dwarf galaxies (Aoki et al. 2009; Cohen & Huang 2009; Frebel et al. 2009).

Finally, we studied the chemical evolution of local ellipticals. Our results were compared with the available observations, which represent the average stellar abundances in local early-type galaxies. Concerning the [$\alpha$/Fe] versus $\sigma$ plot, the observations indicate a positive correlation between [$\alpha$/Fe] and $\sigma$, usually interpreted in terms of more efficient SF efficiency in larger galaxies (Matteucci 1994; Thomas et al. 2005). Previous attempts to reproduce the observations in early-type galaxies by means of semi-analytical $\Lambda$CDM galaxy formation models have led to several unsuccesses. Theoretical results by various authors point towards an anticorrelation between $\alpha$/Fe and $\sigma$ (Thomas 1999; Nagashima et al. 2005).

We have performed a detailed study of the role of various ingredients in determining the slope and the zero-point of the $\alpha$/Fe–$\sigma$ relation. Our predictions computed with a constant Salpeter IMF indicate a flat [$\alpha$/Fe]–$\sigma$. We have found that, by assuming a SF-dependent IMF, Salpeter like (i.e. with slope $x = 1.35$) in objects with SFR $< 100\,{\rm M}_{\odot}\,{\rm yr}^{-1}$ and slightly flatter (with $x = 1$) in systems with strong SF, the observed correlation can be accounted for, at least on the velocity dispersion range $1.8 \leq \log(\sigma/{\rm km\,s}^{-1}) \leq 2.2$. A major role is played by starburst-triggered interactions and AGN feedback. In fact, we have seen that when we relax any of these two ingredients in our models, we predict a flatter [$\alpha$/Fe]–$\sigma$ relation than the one produced considering both effects and the SF-dependent IMF. Our main result is then that, in order to reproduce this correlation, all these three ingredients must be taken into account. The discrepancy between our predicted [$\alpha$/Fe]–$\sigma$ relation and the observations for $\log(\sigma/{\rm km\,s}^{-1}) > 2.3$ may be due to the fact that, at the present stage, the integrated stellar [$\alpha$/Fe] have been computed by considering the integral SF histories of early-type galaxies, and not the contributions of the single progenitors. Since in general the most massive progenitors should exhibit the highest stellar [$\alpha$/Fe] and have a higher weight in the calculation of the total [$\alpha$/Fe], a more detailed computation of the stellar [$\alpha$/Fe] values taking into account each single progenitor could further steepen the predicted [$\alpha$/Fe]–$\sigma$ relation and alleviate the discrepancy for the largest mass systems. This task requires long computational times and will be the subject of a forthcoming paper. With a standard Salpeter IMF, we cannot reproduce the slope of the mass–stellar metallicity relation observed in ellipticals, which should however be considered a less robust observational constraint, mainly owing to a possible template bias affecting the stellar population models used to determine the metallicities. However, we have shown that, also in this case, the assumption of a SF-dependent IMF alleviates the discrepancy between our predictions and the observational data.

In the future, our SAM for galaxy formation will be used to perform a more thorough study of the abundance ratios in ellipticals and of the mass–metallicity relation and its evolution (Calura et al. 2009).

## ACKNOWLEDGMENTS

We wish to thank S. Recchi, G. Cescutti, F. Matteucci and G. De Lucia for several stimulating discussions. G. Lanfranchi and E. Colavitti are acknowledged for providing us with compilations of observational data for the Milky Way and for local dwarf spheroidal galaxies. An anonymous referee is acknowledged for useful suggestions and for a careful reading of the paper. This work was partially supported by the Italian Space Agency through contract ASI-INAF I/016/07/0. FC acknowledges financial support from PRIN2007, Prot.2007JJC53X_001.

## REFERENCES

Alibes A., Labay J., Canal R., 2001, A&A, 370, 1103
Aoki W. et al., 2009, A&A, 502, 569
Arrigoni M., Trager S. C., Somerville R. S., Gibson B. K., 2009, MNRAS, submitted (arXiv:0905.4189)
Ballero S. K., Matteucci F., Ciotti L., Calura F., Padovani P., 2008, A&A, 478, 335
Bellazzini M., Ferraro F. R., Origlia L., Pancino E., Monaco L., Oliva E., 2002, AJ, 124, 3222
Boissier S., Prantzos N., 1999, MNRAS, 307, 857
Bond J. R., Cole S., Efstathiou G., Kaiser N., 1991, ApJ, 379, 440
Calura F., Matteucci F., 2006, ApJ, 652, 889
Calura F., Jimenez R., Panter B., Matteucci F., Heavens A. F., 2008a, ApJ, 682, 252
Calura F., Lanfranchi G. A., Matteucci F., 2008b, A&A, 484, 107
Calura F., Pipino A., Matteucci F., Chiappini C., Maiolino R., Menci N., 2009, in AIP Conf. Proc. Vol. 1111, Probing Stellar Populations out to the Distant Universe: CEFALU 2008. Am. Inst. Phys., New York, pp. 151–154
Carbon D. F., Barbuy B., Kraft R. P., Friel E. D., Suntzeff N. B., 1987, PASP, 99, 335
Carroll B. W., Ostlie D. A., 1996, An Introduction to Modern Astrophysics. Addison-Wesley, San Francisco
Cavaliere A., Vittorini V., 2000, ApJ, 543, 599
Cavaliere A., Lapi A., Menci N., 2002, ApJ, 581, L1
Cayrel R. et al., 2004, A&A, 416, 1117
Cescutti G., 2008, A&A, 481, 691
Chartas G., Brandt W. N., Gallagher S. C., Garmire G. P., 2002, ApJ, 579, 169
Chiappini C., Matteucci F., Romano D., 2001, ApJ, 554, 1044
Clegg R. E. S., Lambert D. L., Tomkin J., 1981, ApJ, 250, 262
Cohen J. G., Huang W., 2009, ApJ, 701, 1053
Colavitti E., Matteucci F., Murante G., 2008, A&A, 483, 401
Dabringhausen J., Kroupa P., Baumgardt H., 2009, MNRAS, 394, 1529
Dekel A., Birnboim Y., 2006, MNRAS, 368, 2
Dekel A., Silk J., 1986, ApJ, 303, 39
De Lucia G., Helmi A., 2008, MNRAS, 391, 14

De Lucia G., Springel V., White S. D. M., Croton D., Kauffman G., 2006, MNRAS, 366, 499
D'Ercole A., Brighenti F., 1999, MNRAS, 309, 941
De Rossi M. E., Tissera P. B., De Lucia G., Kauffmann G., 2009, MNRAS, 395, 210
Di Matteo T., Springel V., Hernquist L., 2005, Nat, 433, 604
Dolphin A. E., Weisz D. R., Skillman E. D., Holtzman J. A., 2005, in Valls-Gabuad D., Chavez M., eds, ASP Conf. Ser., Resolved Stellar Populations. Astron. Soc. Pac., San Francisco, to appear (astro-ph/0506430)
Elmegreen B. G., 2009, in Sheth K., Noriega-Crespo A., Ingalls J., Paladini R., eds, The Evolving ISM in the Milky Way and Nearby Galaxies. http://ssc.spitzer.caltech.edu/mtgs/ismevol/, arXiv:0803.3154
Ferrara A., Pettini M., Shchekinov Y., 2000, MNRAS, 319, 539
François P., Matteucci F., Cayrel R., Spite M., Spite F., Chiappini C., 2004, A&A, 421, 613
Frebel A., Simon J. D., Geha M., Willman B., 2009, ApJ, submitted (arXiv:0902.2395)
Gibson B. K., Matteucci F., 1997, MNRAS, 291, 8
Gilmore G., Wyse R. F. G., Norris J. E., 2002, ApJ, 574, L39
Greggio L., 1997, MNRAS, 285, 151
Greggio L., 2005, A&A, 441, 1055
Hernandez X., Gilmore G., Valls-Gabaud D., 2000, MNRAS, 317, 831
Hernandez X., Avila-Reese V., Firmani C., 2001, MNRAS, 327, 329
Ikuta C., Arimoto N., 2002, A&A, 391, 55
Israelian G., Ecuvillon A., Rebolo R., García-López R., Bonifacio P., Molaro P., 2004, A&A, 421, 649
Iwamoto K., Brachwitz F., Nomoto K., Kishimoto N., Umeda H., Hix W. R., Thielemann F.-K., 1999, ApJS, 125, 439
Jorgensen B. R., 2000, A&A, 363, 947
Kauffmann G., 1996, MNRAS, 281, 475
Kauffmann G., Charlot S., 1998, MNRAS, 294, 705
Kennicutt R. C., 1998, ApJ, 327, 541
Kroupa P., 2002, Sci, 295, 82
Kroupa P., Tout C. A., Gilmore G., 1993, MNRAS, 262, 545
Lacey C., Cole S., 1993, MNRAS, 262, 627
Laird J. B., 1985a, ApJS, 57, 389
Laird J. B., 1985b, ApJ, 289, 556
Lanfranchi G., Matteucci F., 2003, MNRAS, 345, 71
Lanfranchi G., Matteucci F., 2004, MNRAS, 351, 1338
Lanfranchi G., Matteucci F., 2007, A&A, 468, 927
Lanfranchi G., Matteucci F., Cescutti G., 2006, A&A, 453, 67
Lapi A., Cavaliere A., Menci N., 2005, ApJ, 619, 60
Mac Low M.-M., Ferrara A., 1999, ApJ, 513, 142
Maiolino R. et al., 2008, A&A, 488, 463
Mannucci F., Della Valle M., Panagia N., 2006, MNRAS, 370, 773
Maoz D., 2008, MNRAS, 384, 267
Marcolini A., D'Ercole A., Battaglia G., Gibson B. K., 2008, MNRAS, 386, 2173
Marconi G., Matteucci F., Tosi M., 1994, MNRAS, 270, 35
Martin C. L., 2005, ApJ, 621, 227
Martin C. L., Kobulnicky H. A., Heckman T. M., 2002, ApJ, 574, 663
Mateo M. L., 1998, ARA&A, 36, 435
Matteucci F., 1994, A&A, 288, 57
Matteucci F., 2001, The Chemical Evolution of the Galaxy. ASSL, Kluwer, Dordrecht
Matteucci F., Greggio L., 1986, A&A, 154, 279
Matteucci F., Recchi S., 2001, ApJ, 558, 351
Matteucci F., Ponzone R., Gibson B. K., 1998, A&A, 335, 855
Matteucci F., Panagia N., Pipino A., Mannucci F., Recchi S., Della Valle M., 2006, MNRAS, 372, 265
Menci N., Cavaliere A., Fontana A., Giallongo E., Poli F., 2002, ApJ, 575, 18
Menci N., Cavaliere A., Fontana A., Giallongo E., Poli F., Vittorini V., 2004, ApJ, 604, 12
Menci N., Fontana A., Giallongo E., Salimbeni S., 2005, ApJ, 632, 49
Menci N., Fontana A., Giallongo E., Grazian A., Salimbeni S., 2006, ApJ, 647, 753
Menci N., Fiore F., Puccetti S., Cavaliere A., 2008, ApJ, 686, 219
Mera D., Chabrier G., Schaeffer R., 1998, A&A, 330, 953
Naab T., Ostriker J. P., 2006, MNRAS, 366, 899
Nagashima M., Okamoto T., 2006, ApJ, 643, 863
Nagashima M., Lacey C. G., Okamoto T., Baugh C. M., Frenk C. S., Cole S., 2005, MNRAS, 363, L31
Ott J., Walter F., Brinks E., 2005, MNRAS, 358, 1453
Pilyugin L. S., 1993, A&A, 277, 42
Pipino A., Devriendt J. E. G., Thomas D., Silk J., Kaviraj S., 2008, preprint (astro-ph/0810.5753)
Portinari L., Moretti A., Chiosi C., Sommer-Larsen J., 2004, ApJ, 604, 579
Pounds K., King A. R., Page K. L., O'Brien P. T., 2003, MNRAS, 346, 1025
Prantzos N., Silk J., 1998, ApJ, 507, 229
Proctor R. N., Forbes D. A., Hau G. K. T., Beasley M. A., De Silva G. M., Contreras R., Terlevich A. I., 2004, MNRAS, 349, 1381
Proga D., 2007, ApJ, 661, 693
Recchi S., Matteucci F., D'Ercole A., 2001, MNRAS, 322, 800
Recchi S., Hensler G., Angeretti L., Matteucci F., 2006, A&A, 445, 875
Recchi S., Spitoni E., Matteucci F., Lanfranchi G. A., 2008, A&A, 489, 555
Recchi S., Calura F., Kroupa P., 2009, A&A, 499, 711
Reshetnikov V. P., 2000, Astrophysics, 43, 145
Ripamonti E., Tolstoy E., Helmi A., Battaglia G., Abel T., 2007, EAS Publ. Ser., 24, 15
Risaliti G., Bianchi S., Matt G., Baldi A., Elvis M., Fabbiano G., Zezas A., 2005, ApJ, 630, L129
Roberts M. S., Haynes M. P., 1994, ARA&A, 32, 115
Rocha-Pinto H. J., Maciel W. J., 1996, MNRAS, 279, 447
Romano D., Chiappini C., Matteucci F., Tosi M., 2005, A&A, 430, 491
Rupke D. S., Veilleux S., Sanders D. B., 2005, ApJ, 632, 751
Salpeter E. E., 1955, ApJ, 121, 161
Salvadori S., Ferrara A., Schneider R., 2008, MNRAS, 386, 348
Sawala T., Scannapieco C., White S. D. M., 2009, preprint (arXiv:0902.1754)
Somerville R. S., Primack J. R., 1999, MNRAS, 310, 1087
Spergel D. N. et al., 2007, ApJS, 170, 377
Spite M. et al., 2005, A&A, 430, 655
Sullivan M. et al., 2006, ApJ, 648, 868
Thomas D., 1999, MNRAS, 306, 655
Thomas D., Greggio L., Bender R., 1999, MNRAS, 302, 537
Thomas D., Maraston C., Bender R., Mendes de Oliveira C., 2005, ApJ, 621, 673
Timmes F. X., Woosley S. E., Weaver T. A., 1995, ApJS, 98, 617
Tomkin J., Woolf V. M., Lambert D. L., Lemke M., 1995, AJ, 109, 2204
Turnshek D. A., Grillmair C. J., Foltz C. B., Weymann R. J., 1988, ApJ, 325, 651
Valiante R., Matteucci F., Recchi S., Calura F., 2009, New Astron. 14, 638
van den Bergh S., 1994, ApJ, 428, 617
van den Bergh S., Tammann G. A., 1991, ARA&A, 29, 363
van den Hoek L. B., Groenewegen M. A. T., 1997, A&AS, 123, 305
Veilleux S., Cecil G., Bland-Hawthorn J., 2005, ARA&A, 43, 769
Weymann R. J., 1981, ARA&A, 19, 41
Whelan J., Iben I., Jr, 1973, ApJ, 186, 1007
Woo J., Courteau S., Dekel A., 2008, MNRAS, 390, 1453
Woosley S. E., Weaver T. A., 1995, ApJS, 101, 181
Wyse R. G., 2009, Int. Astron. Union Symp., 254, 179
Wyse R. F. G., Gilmore G., 1995, AJ, 110, 2771

This paper has been typeset from a TEX/LATEX file prepared by the author.